Comparative Biochemistry and Physiology Part B: Biochemistry and Molecular Biology
April 2015, Volume 182 Pages 14-26
http://dx.doi.org/10.1016/j.cbpb.2014.11.011
http://archimer.ifremer.fr/doc/00240/35173/

Molecular and functional characterization of seven Na+/K+-ATPase β subunit paralogs in Senegalese sole (*Solea senegalensis* Kaup, 1858)

Armesto Paula [1], Infante Carlos [2], Cousin Xavier [3], Ponce Marian [1], Manchado Manuel [1, *]

[1] IFAPA Centro El Toruño, 11500 El Puerto de Santa María (Cádiz), Spain
[2] Fitoplancton Marino, S.L. Dársena Comercial s/n (Muelle Pesquero). 11500 El Puerto de Santa María (Cádiz), Spain
[3] Ifremer, Laboratoire d'Ecotoxicologie, Place Gaby Coll, BP 7, 17137 L'Houmeau, France

* Corresponding author : Manuel Manchado, Tel.: + 34 956011334 ; fax: + 34 956011324 ; email address : manuel.manchado@juntadeandalucia.es

Abstract :

In the present work, seven genes encoding Na+,K+-ATPase (NKA) β-subunits in the teleost Solea senegalensis are described for the first time. Sequence analysis of the predicted polypeptides revealed a high degree of conservation with those of other vertebrate species and maintenance of important motifs involved in structure and function. Phylogenetic analysis clustered the seven genes into four main clades: β1 (atp1b1a and atp1b1b), β2 (atp1b2a and atp1b2b), β3 (atp1b3a and atp1b3b) and β4 (atp1b4). In juveniles, all paralogous transcripts were detected in the nine tissues examined albeit with different expression patterns. The most ubiquitous expressed gene was atp1b1a whereas atp1b1b was mainly detected in osmoregulatory organs (gill, kidney and intestine), and atp1b2a, atp1b2b, atp1b3a, atp1b3b and atp1b4 in brain. An expression analysis in three brain regions and pituitary revealed that β1-type transcripts were more abundant in pituitary than the other β paralogs with slight differences between brain regions. Quantification of mRNA abundance in gills after a salinity challenge showed an activation of atp1b1a and atp1b1b at high salinity water (60 ppt) and atp1b3a and atp1b3b in response to low salinity (5 ppt). Transcriptional analysis during larval development showed specific expression patterns for each paralog. Moreover, no differences in the expression profiles between larvae cultivated at 10 and 35 ppt were observed except for atp1b4 with higher mRNA levels at 10 than 35 ppt at 18 days post hatch. Whole-mount in situ hybridization analysis revealed that atp1b1b was mainly localized in gut, pronephric tubule, gill, otic vesicle, and chordacentrum of newly hatched larvae. All these data suggest distinct roles of NKA β subunits in tissues, during development and osmoregulation with β1 subunits involved in the adaptation to hyperosmotic conditions and β3 subunits to hypoosmotic environments.

Abbreviations

- aa, amino acid;
- bp, base pair;
- cDNA, DNA complementary to RNA;
- CDS, coding sequence;
- dph, days post hatch;
- DEPC, diethyl pyrocarbonate;
- ECD, extracellular domain;
- ICD, intracellular domain;
- WISH, whole-mount *in situ* hybridization;
- kb, kilobase(s);
- NKA, Na^+,K^+-ATPase;
- nt, nucleotide(s);
- PBS, phosphate buffered saline;
- ppt, parts per thousand;
- SEM, standard error of the mean;
- TMD, transmembrane domain

Keywords : Senegalese sole, Na+,K+-ATPase, Beta subunit, Paralogs, Osmoregulation

1. Introduction

The Na^+,K^+ ATPase (NKA) plays a primary role in the active ion transport and osmoregulatory capacity of euryhaline fish (Cutler et al., 1995; Cutler et al., 1997a; McCormick et al., 2009). This enzyme belongs to the P-type ATPase family of cation pumps that couples the exchange of two extracellular K^+ ions for three intracellular Na^+ ions, a process that requires the hydrolysis of one molecule of ATP (Lingrel and Kuntzweiler, 1994; Blanco and Mercer, 1998; Mobasheri et al., 2000; Bensimon-Brito et al., 2012). This transporter, as well as its close homolog the gastric H^+,K^+-ATPase, requires a β subunit at equimolar amounts to the catalytic α subunit to become functional NKA αβ heterodimers or conform oligomers of multiple heterodimer units (Linnertz et al., 1998; Taniguchi et al., 2001; Laughery et al., 2004). The structure of the NKA β subunits consists of an amino terminal cytoplasmic tail, a single transmembrane domain, and a large and highly glycosylated ectodomain with conserved disulfide bridge-forming cysteine residues (Martin-Vasallo et al., 1989; Blanco, 2005; Durr et al., 2009). These β subunits primary act as chaperone molecules contributing to the proper folding and protection of α subunits as well as to the anchoring and integration of heterodimers into the plasma membrane (Geering, 1991; Laughery et al., 2003). Moreover, the β subunits also modulate NKA transport activity by affecting whole enzyme stability, α subunit cation affinity and K^+ occlusion (Lutsenko and Kaplan, 1993; Geering et al., 1996; Hasler et al., 1998; Geering, 2008; Durr et al., 2009). Other functions of β subunits include the maintenance of intercellular junctions throughout β1-β1 intercellular bridges facilitating cell polarity, transepithelial transport (Rajasekaran et al., 2001a; Rajasekaran et al., 2001b; Vagin et al., 2012) and adhesion of glial cells (β2-type subunit)(Antonicek and Schachner, 1988; Gloor et al., 1990; Muller-Husmann et al., 1993).

Four β-subunit isoforms have been described in fish and mammals (Mobasheri et al., 2000; Blanco, 2005). These subunits are encoded by up to seven distinct paralogs (two β1, two β2, two β3 and one β4) in zebrafish (Rajarao et al., 2001; Canfield et al., 2002; Pestov et al., 2007) and six (two β1, two β2, and two β3) in Atlantic salmon (Gharbi et al., 2005). These paralogous genes exhibit distinct expression patterns in tissues and developmental stages depending on the species (Cutler et al., 1995; Cutler et al., 1997b; Rajarao et al., 2001; Rajarao et al., 2002). But, in general, β1-type subunits are widely detected in several tissues and, particularly, in those organs involved in osmoregulation in fish. The β2- and β3-type subunits are mainly expressed in nervous tissues although β3 is also highly expressed in testis (Cutler et al., 1995; Cutler et al., 1997b; Mobasheri et al., 2000; Rajarao et al., 2001; Rajarao et al., 2002). This tissue-specific distribution pattern indicates that paralogs have followed a subfunctionalization or even a neofunctionalization process during evolution. In fact, some studies have demonstrated that β4 subunit only associates to α subunits to produce functional ion pumps in non-mammalian species showing distinct expression profiles and cellular functions in fish and mammals (Mobasheri et al., 2000; Blanco, 2005; Pestov et al., 2007). Moreover, tissue-specific distribution pattern for α and β paralogs is very important as it determines the αβ combination of the NKA holoenzyme and, hence, its structure, kinetic properties and functional capabilities (Sweadner, 1985; Shyjan et al., 1990; Lingrel and Kuntzweiler, 1994; Blanco et al., 1995; Chow and Forte, 1995; Crambert et al., 2000; Mobasheri et al., 2000; Rajarao et al., 2001; Canfield et al., 2002; Blanco, 2005; Blasiole et al., 2006). The α1β1 combination is considered as the most ubiquitous NKA isozyme and the predominant heterodimer of kidney and teleosts gills participating in primary ion uptake or secretion during environmental salinity adaptation

(Cutler et al., 1995; Cutler et al., 2000; Blanco, 2005; Nilsen et al., 2007; Liao et al., 2009).

The Senegalese sole (*Solea senegalensis* Kaup 1858) is an economically important species both in fisheries and aquaculture. This species is partially euryhaline and can cope with wide fluctuations of external salinity by adjusting energy allocation, NKA activity and cortisol levels (Arjona et al., 2007; Herrera et al., 2012). During development, larvae adapt successfully to low salinities after mouth opening (3 days post hatch, dph) exhibiting similar growth rates when they are cultivated between 10-33 ppt (Salas-Leiton et al., 2012). In contrast, severe jaw malformations occur when embryos and newly hatched larvae are incubated at 10 ppt or lower salinities (Salas-Leiton et al., 2012). Recently, a set of five paralogous genes encoding the NKA α subunits has been described in sole (Armesto et al., 2014). They exhibited tissue and developmental specific expression patterns. Moreover, *atp1a1a* was identified as the main osmoregulatory paralog due to its high steady-state mRNA levels in osmoregulatory organs and its transcriptional response to hypersalinity in gills (Armesto et al., 2014). Yet, little information is available about NKA β subunit regulation and distribution in Senegalese sole. Previous studies in fish have shown that β subunits are transcriptionally regulated by environmental salinity and developmental stage (Cutler et al., 2000; Nilsen et al., 2007). Moreover, their expression is tightly regulated at transcriptional and translational levels by several hormones involved in osmoregulation (Deane and Woo, 2005). Due to the central role of these β subunits to modulate the NKA holoenzyme activity, a better characterization of the set of genes encoding β subunit as well as their transcriptional responses after a salinity shift and during development is required to understand osmoregulatory responses in sole.

The aims of this work were: 1) identification and characterization of NKA β subunits in sole, 2) establishment of the relative mRNA abundance of NKA β subunits in juvenile tissues and during larval development, 3) evaluation of transcriptional responses to salinity challenge in tissues of juveniles, and 4) mapping the change in the NKA β subunits transcript amounts in newly hatched and developing larvae under a salinity challenge.

2. Materials and methods

2.1 Source of fish and experimental rearing conditions

Tissue samples from Juvenile Senegalese sole were those reported previously (Manchado et al., 2008b, 2009). Briefly, individuals (average weight=23.2±3.6 g; n=3) were obtained from IFAPA Centro *El Toruño* facilities (El Puerto Santa María, Cádiz, Spain). They were sacrificed by immersion in 2-phenoxyetanol (300 ppm for 10 min). Liver, spleen, brain, gills, intestine, kidney, heart, skeletal muscle, and skin were rapidly dissected out, frozen in liquid nitrogen, and stored at -80 °C until use.

To characterize the distribution of the seven NKA β paralogs in different brain sections, 18 adult soles (average weight: 1,747±547 g) were euthanized using 2-phenoxyetanol (same dose as indicated above). Brain was rapidly dissected out and pituitary, hypothalamus, optic tectum and telencephalon were separated, frozen in liquid nitrogen, and stored at -80 °C until use. Prior to RNA isolation, brain regions from different individuals were pooled without considering sex to produce three independent samples for qPCR analysis.

137 To study the effect of osmotic conditions on mRNA abundance of the NKA β
138 paralogs, 150 juveniles (mean weight = 29.9±0.8 g) were acclimated in a rectangular 4
139 m^3 tank. Temperature ranged between 17.6-18.3 ºC and salinity oscillated between
140 35.0-35.4 ppt. Ten days before experiment started, the temperature was reduced to 16.5
141 ºC (ranging 16-17 ºC) to fit better the environmental temperature conditions (January-
142 February 2008). During this acclimation period, animals were fed dry pellets (LE2 Elite,
143 Skretting, Burgos, Spain) provided by automatic feeders (approx. 1% biomass daily).
144 Soles were maintained in a flow-through circuit under automatic control of temperature
145 with 300% daily water renewal. Water supply was from the so-called "Rio San Pedro"
146 at El Puerto Santa María (Cádiz), an arm of the sea with a length of 12 km affected by a
147 semi-diurnal tidal with a typical seawater composition (Martínez-Velasco et al., 1999).
148 Pumping station was located approximately in the middle of the river near the sampling
149 station number 7 as described previously (Tovar et al., 2000) . Before starting
150 experiment, animals were distributed in six 100 L tanks (25 soles per tank) at a salinity
151 of 35 ppt (35.0-35.3 ppt) under a natural photoperiod. After an acclimation period (24
152 h), water was completely replaced in less than half an hour establishing three different
153 salinities in duplicate tanks: low-salinity water (5 ppt), control (35 ppt) and high-salinity
154 water (60 ppt). Expected experimental salinities (low-salinity, control and high-salinity)
155 were achieved by mixing seawater with dechlorinated tap water or marine salt
156 depending on the condition. No food was provided during the experiment. Two
157 individuals from each tank were initially sampled before salinity change (0 h); then
158 three individuals per tank were sampled at 24, 48, 72, 96 and 168 h (7 d) after salinity
159 change. Animals were euthanized by phenoxyethanol overdose (300 ppm for 10 min).
160 Gills were rapidly dissected out, frozen in liquid nitrogen and stored at -80°C.

161 To evaluate the effect of low salinity on mRNA levels of NKA β paralogs

during larval development, 1 dph larvae (November 2011) were obtained from Pesquerías Isla Mayor, S.A. (Isla Mayor, Seville). After transporting to IFAPA Centro *El Toruño* facilities, larvae were acclimated during 1 hour at 19ºC before distributing in six 300 L tanks at an initial density of 30 to 35 larvae L^{-1}. At 3 dph, after confirming that more than 90% of the larvae in each tank had opened the mouth, salinity was progressively reduced in three tanks to establish a final salinity of 10 ppt in approximately 12 h. The other three tanks were kept as controls at 35 ppt. Temperature was maintained between 18.5-19 ºC during the experiment with a 16L:8D photoperiod and light intensity of 300 lux. Larvae were fed rotifers (*Brachionus plicatilis*), previously enriched with *Isochrysis galbana* (T-ISO strain) cultivated at exponential phase, from 3 until 9 dph. T-ISO cells were also added (2 mg dry weight L^{-1} d^{-1}) directly to the larval culture tanks during the rotifer feeding stage. From 7 dph until the end of the experiment sole larvae were fed *Artemia* metanauplii enriched with T-ISO. Sole larvae were sampled on 3, 8, 15, 21 and 25 dph for growth and metamorphosis progress monitoring. In each sampling, three independent pools per tank were randomly collected. Each pool (from 10 to 100 larvae depending on the age) was collected using a 350-µm-mesh net, washed with DEPC water, placed in separate Eppendorf tubes, frozen in liquid nitrogen and stored at -80°C until analysis.

Dry weight and metamorphic stages were determined as previously described (Fernandez-Diaz et al., 2001; Manchado et al., 2008a; Salas-Leiton et al., 2012). Metamorphic index was calculated as follows: [(S1 larvae x1) + (S2 larvae x2) + (S3 larvae x3) + (S4 larvae x4)]/total number of larvae, where S1-S4 indicate the number of larvae in such specific metamorphic stage. The larval survival percentage was calculated at the end of the experiment (25 dph).

To evaluate the effect of low salinity on mRNA levels of NKA β paralogs during early developmental stages, eggs from natural spawn were collected and fertilized eggs separated by buoyancy as described above. After that, embryos (in gastrula stage) were incubated at two salinities (10 and 35 ppt) in 15 L cylinder conical tubes coupled to a recirculation system to keep constant temperature (20 ºC) and target salinities. Initial culture density was 1,500-2,000 embryos L^{-1}, and experiment was performed in duplicate tanks. At 1, 2 and 3 dph, three pools of larvae were collected from each tank as described above, washed with DEPC water, directly frozen in liquid nitrogen and separately stored at -80 °C until analysis. In addition, some larvae were fixed overnight in 4% paraformaldehyde at 4ºC for whole-mount in situ hybridization (WISH) analysis.

2.2 Sequencing of Senegalese sole atp1b1a, atp1b1b, atp1b2a, atp1b2b, atp1b3a, atp1b3b and atp1b4

Partial coding sequences of Senegalese sole *atp1b1a* and *atp1b1b* were obtained from EST libraries built in the Pleurogene project (Cerda et al., 2008). Moreover, additional partial sequences of *atp1b1a*, *atp1b1b*, *atp1b2a*, *atp1b2b*, *atp1b3a*, *atp1b3b* and *atp1b4* were obtained from unigenes produced in the AQUAGENET project and hosted at SoleaDB (Benzekri et al., 2014). Partial unigene nucleotide sequences were assembled using Seqman *v*5.53 (Lasergene, DNASTAR Inc., Madison, MI, USA) to confirm paralog sequences. To warrant sequence reliability, only those assemblies with three or more overlapping unigenes with 99% minimal identity were considered. Nucleotide sequences identity of the sequenced cDNA was confirmed by Blasting against the NCBI database.

Predicted NKA β amino acid sequences were determined with EditSeq *v*8.1.3 software (Lasergene, DNASTAR, Inc., Madison, MI, USA). The Motif Scan tool (Pagni et al., 2007) and TMpred tool (Hofmann and Stoffel, 1993) at ExPASy portal were used to identify domains in the predicted NKA β protein sequences. NKA β cDNA sequences of diverse chordates were retrieved from GenBank/EMBL/DDBJ and Ensembl (http://www.ensembl.org/index.html) and used for multiple sequence alignments and phylogenetic analyses (Additional file 1). Sequence alignment and identities estimation were performed using MegAlign software (Lasergene, DNASTAR, Inc., Madison, MI, USA). Maximum likelihood phylogenetic analysis was performed and the best-fit model of sequence evolution was determined to be WAG+G (-lnL = -31112.20) using the ProtTest *v*2.4 (Abascal et al., 2005) with a gamma distribution shape parameter (four rate categories) of 1.465. The PHYLIP package (Felsenstein, 1989) was then employed to estimate the bootstrap values using SEQBOOT (1000 replicates) and the data were analyzed using the software PHYML (Guindon et al., 2010). The consensus phylogenetic tree was then obtained (CONSENSE). Trees were drawn using the TreeViewX program *v*0.5.0 (Page, 1996). The *Ciona intestinalis* atpase sequence (Ensembl accession no. **ENSCING00000023552**) was used as an outgroup to root the tree.

2.3 RNA isolation and gene expression analysis

Homogenization of juvenile tissues, brain and larvae was carried out using the Lysing Matrix D (Q-BioGene, Heidelberg, Germany) for 40 s at speed setting 6 in the FastPrep-24^{TM} Instrument (MP Biomedicals, Santa Ana, CA, USA). Total RNA was isolated from 50 mg of tissues or pooled larvae using the RNeasy Mini Kit (Qiagen, Valencia, CA, USA). For skeletal muscle, heart and skin the RNeasy Fibrous Tissue

233 Mini Kit (Qiagen, Valencia, CA, USA) was used whereas for brain regions and pituitary
234 pools the RNeasy Lipid Tissue Mini Kit (Qiagen, Valencia, CA, USA). All RNA
235 isolation procedures were performed in accordance with the manufacturer's protocol. In
236 all cases, total RNA was treated twice with DNase I using the RNase-Free DNase kit
237 (Qiagen, Valencia, CA, USA) for 30 min to avoid amplification of genomic DNA. RNA
238 sample quality was checked in agarose gels and quantification was performed with a
239 NanoDrop 8000 spectrophotometer (Thermo Fisher Scientific Inc., Wilmington, DE,
240 USA). Average 260/280 ratio was 2.03 and 260/230 was 2.0. Total RNA (1 μg) from
241 each sample was reverse-transcribed with the iScript™ cDNA Synthesis kit (Bio-Rad,
242 Hercules, CA, USA) following the manufacturer's protocol. Lack of genomic DNA
243 contamination was confirmed by PCR amplification of RNA samples in the absence of
244 cDNA synthesis.

245 Real-time analysis was carried out on a CFX96™ Real-Time System (Bio-Rad,
246 Hercules, CA, USA) using Senegalese sole specific primers for each NKA β transcript
247 (Table 1). Real-time reactions were accomplished in a 10-μl volume containing cDNA
248 generated from 10 ng of original RNA template, 300 nM each of specific forward and
249 reverse primers, and 5 μl of iQ™ SYBR Green Supermix (Bio-Rad, Hercules, CA,
250 USA) The amplification protocol used was as follows: initial 7 min denaturation and
251 enzyme activation at 95 ºC, 40 cycles of 95 ºC for 15 s and 70 ºC for 30 s. Each qPCR
252 assay was performed in duplicate. For normalization of cDNA loading, all samples were
253 run in parallel with the reference genes glyceraldehyde-3-phosphate dehydrogenase
254 (*gapdh2*; embryos), 18S rRNA (juvenile tissues) or ubiquitin (*ub52*; salinity challenge
255 and brain in juveniles) which have been previously demonstrated to be suitable as
256 reference genes for these samples (Manchado et al., 2007; Infante et al., 2008). For
257 larvae cultured at two salinities, expression of target genes were normalized using

geometric mean of *ub52* and *gapdh2* (Vandesompele et al., 2002; Infante et al., 2008). Reference genes for normalization were selected according to their expression stability within each experiment. To estimate efficiency, a standard curve was generated for each primer pair based on 10-fold serial dilutions corresponding to cDNA transcribed from 100 to 0.01 ng of total RNA. Calibration curves exhibited a correlation coefficient higher than 0.99, and the corresponding real-time PCR efficiencies (E) were 1.98, 1.92, 2.04, 2.0, 2.01, 2.00 and 2.05 for *atp1b1a*, *atp1b1b*, *atp1b2a*, *atp1b2b*, *atp1b3a*, *atp1b3b* and *atp1b4*, respectively. Relative mRNA expression was determined using the $2^{-(\Delta\Delta Ct)}$ method (Livak and Schmittgen, 2001; Manchado et al., 2007). Samples corresponding to spleen and pituitary were used as a calibrator in tissues and brain regions gene expression experiments, respectively. For salinity challenge experiments, the calibrators were the 35 ppt group at 24h after salinity change in gills, 1 dph larvae from embryos incubated at 10 ppt and 3 dph larvae cultivated at 10 ppt. Results were expressed as mean ± SEM.

2.4 Whole mount in situ hybridization (WISH)

To synthetize the ISH probe for *atp1b1b*, a PCR fragment of 731 bp was amplified using specific primers (5'- CCTCTGTGTATTGCTGCCTCGT -3' (F) and 5'-CGAGTCGAGACACTGACTTTAGCAC-3' (R)). The PCR product was cloned in TOPO-TA vector and a sense and anti-sense probe were synthesized using 20 U T3 and T7 polymerase in transcription buffer (Promega, Madison, WI, USA) with 1 µl digoxigenin-RNA labeling mix (Roche Diagnostics, Mannheim, Germany) as described in Thisse and Thisse (2008).

For WISH analyses in new-hatched larvae, samples were fixed in 4% (wt/vol) paraformaldehyde in 1X PBS overnight at 4 ºC, dehydrated in methanol 100% and

conserved at -20ºC until processing. Fixed embryos were depigmented and permeabilized (10µg/ml proteinase K (Sigma-Aldrich, St. Louis, MO, USA) for 16 min at 37ºC) before being soaked in the digoxigenin-labeled *atp1b1b* probe as previously described (Thisse and Thisse, 2008). Excess probe was then removed according to the same protocol through successive washes in 2XSaline-sodium citrate (SSC) buffer and 0.2XSSC at 70°C and a last wash in 1XPBT. Hybrids were detected using anti-DIG serum (1/5000; Roche Diagnostics, Mannheim, Germany) and developed using the chromogens NBT/BCIP (Roche Diagnostics, Mannheim, Germany). Embryos were photographed in 80% glycerol using an Olympus SZX9 (Olympus Europa Holding GmbH, Hamburg, Germany) dissecting microscope and DFK31AU03 camera (The Imaging Source Europe GmbH, Bremen, Germany).

2.5. Statistical analysis

Significant differences during in juvenile tissues and between larvae incubated at different salinities were determined by a Kruskal-Wallis test (non-parametric one-way ANOVA) followed by a Fisher's Least Significant Difference (LSD) test using Statgraphics Plus *v*5.1 software (Statpoint Technologies, Warrenton, USA). For the salinity challenge in juveniles and larvae, changes in mRNA abundance over time and salinity were analyzed by a two-way ANOVA followed by Tukey's post hoc analysis for pair-wise comparisons when applicable. A Kolmogorov-Smirnov normality test was performed to evaluate normality distribution. Statistical analyses were performed with the SPSS *v*21 software (IBM Corp., Armonk, NY, USA) and Statistix 9 (Analytical Software, Tallahassee, FL, USA). Significance was accepted at $p<0.05$.

3. Results

3.1 Molecular characterization and phylogeny of Senegalese sole atp1b1a, atp1b1b, atp1b2a, atp1b2b, atp1b3a, atp1b3b and atp1b4

Seven transcripts encoding Senegalese sole NKA β subunits were sequenced and designated as *atp1b1a, atp1b1b, atp1b2a, atp1b2b, atp1b3a, atp1b3b* and *atp1b4*. One transcript showed a 99% identity with a previous sequence (identified as *atp1b1a*) available at GenBank/EMBL/DDBJ databases (Accession nº JX508625) although phylogenetic analysis (see below) clearly identified this paralog as *atp1b1b*. No sequences corresponding to the other paralogs were identified in public databases. Full-length cDNA sequences were deposited in GenBank/EMBL/DDBJ under accession Nos. AB970472, AB970473, AB970474, AB970475, AB970476, AB970477, AB970478, for Senegalese sole *atp1b1a, atp1b1b, atp1b2a, atp1b2b, atp1b3a, atp1b3b and atp1b4*, respectively.

Open reading frames (ORF) length of NKA β subunits in sole ranged between 843 and 1,029 nucleotides (nt) for *atp1b3a* and *atp1b4*, respectively (Additional file 2). Regarding to structural features, a single transmembrane domain (TMD) was identified in all subunits as predicted by TMpred (Fig. 1). Extracellular domain (ECD), in the C-termini, was the longest domain representing between 65% and 83% of predicted peptide sequence for NKAβ4 and NKAβ1b, respectively. Moreover, intracellular domain (ICD) was longer in NKAβ4 (93 amino acids) than in other NKA β isoforms (from 29 to 46 amino acids for NKAβ2b and NKAβ3b, respectively).

A search for PROSITE patterns identified a NKA β subunit signature 2 in all paralogs (box number 4 in Fig. 1) and signature 1 only in NKAβ1a, NKAβ1b and NKAβ2b (box number 1). Several conserved motifs and residues were identified by

sequence comparison with previous studies (Geering, 2001; Hasler et al., 2001; Shinoda et al., 2009). Three conserved tyrosines (asterisks in Fig. 1) involved in α–β interactions were also identified in all paralogs. Two Tyr residues were located within a cluster of aromatic residues (box number 2) while the third one was localized in the ECD within the YYPYY motif (box number 6). Moreover, the conserved motif LI*XX*G*XXX*G*XXX*G in TMD (box number 3) and an amino acid insertion critical for β1-β1 binding was also identified for NKAβ1a (with a central threonine as in rat) and NKAβ1b (without threonine as in dog) (box number 5). Furthermore, six cysteine residues involved in three conserved disulphide bonds were also located into the ECD. Some potential N-glycosylation sites (from 2 to 5 in NKAβ1a and NKAβ4, respectively) located exclusively in the ECD were also identified.

Sequence identities between Senegalese sole NKA β subunits and orthologous sequences identified in *Danio rerio* and *Oryzias latipes* were estimated (Additional file 3). Identities between *S. senegalensis* NKA β paralogous genes ranged between 30.1% and 64.5% for *atp1b4*/*atp1b1a* and *atp1b1a*/*atp1b1b*, respectively for nucleotide sequences and between 25.6% and 66.7% for *atp1b4*/*atp1b3b* and *atp1b2a*/*atp1b2b*, respectively for amino acid sequences. Comparisons with other teleosts revealed an overall amino acid sequence identity ranging from 25.6% (between Senegalese sole NKAβ4 and *O. latipes* NKAβ1b) to 90.4% (between Senegalese sole NKAβ4 and *O. latipes* NKAβ4). Comparisons of ICD, ECD and TM domain among species showed the lowest sequence identity percentages for N-terminal domain (average 30.8% between Senegalese sole and other teleost species for all NKA β paralogs). The highest amino acid sequence identity was found for TM domain (average 58.6%).

The Maximum Likelihood phylogenetic tree (Fig. 2) showed that *S. senegalensis* NKA β paralogous genes clustered into four major and consistent clades, referred to as β1, β2, β3 and β4, that grouped *atp1b1, atp1b2, atp1b3 and atp1b4* vertebrate orthologous genes. These clades were supported by 100%, 97%, 99% and 99% bootstrap values, respectively. Moreover, a gene duplication for β1, β2 and β3 clades was also identified in Senegalese sole and other Actinopterygii species that clustered into two separate and well-supported clades (referred to as a-type/b-type).

3.2 Transcript levels of atp1b1a, atp1b1b, atp1b2a, atp1b2b, atp1b3a, atp1b3b and atp1b4 in juvenile tissues

Steady-state levels of *atp1b1a, atp1b1b, atp1b2a, atp1b2b, atp1b3a, atp1b3b and atp1b4* transcripts were quantified in nine different tissues from juvenile soles (Fig. 3). Transcript levels of *atp1b1a* were ubiquitous although slightly more abundant in brain and kidney (4.2- and 3.3-fold higher than in spleen, respectively; Fisher's LSD $p<0.05$) followed by heart (2.7-fold higher; Fisher's LSD $p<0.05$). The *atp1b1b* showed the highest mRNA levels in osmoregulatory organs: intestine (254-fold higher than in spleen; Fisher's LSD $p<0.05$), kidney (166-fold higher; Fisher's LSD $p < 0.05$) and gills (113-fold higher; Fisher's LSD $p<0.05$). In contrast, *atp1b2a, atp1b2b, atp1b3a, atp1b3b* and *atp1b4* exhibited the highest transcript levels in brain (518-fold, 70,666-fold, 3,434-fold, 8,624-fold and 20,804-fold higher than in spleen, respectively; Fisher's LSD $p<0.05$).

To confirm the expression of these five NKA β paralogous genes in nervous tissue, we evaluated their steady-state levels in three different sections of adult sole brain and pituitary (Fig. 4). No significant differences were found in *atp1b1a* expression among the four regions examined, while *atp1b1b* transcript levels were slightly higher

375 in optic tectum than hypothalamus and telencephalon (1.4- and 1.3-fold, respectively;
376 Fisher's LSD $p<0.05$). In contrast, *atp1b2a, atp1b2b, atp1b3a, atp1b3b* and *atp1b4*
377 showed the lowest transcript amounts in pituitary while no significant differences
378 between hypothalamus, optic tectum and telencephalon were observed (average mean
379 fold change for the three brain sections were 75-, 69-, 72-, 19- and 36-fold higher than
380 in pituitary for *atp1b2a, atp1b2b, atp1b3a, atp1b3b* and *atp1b4*, respectively).

381 *3.3 Transcript levels of atp1b1a, atp1b1b, atp1b2a, atp1b2b, atp1b3a, atp1b3b and*
382 *atp1b4 during larval development and effect of salinity*

383 To assess the effect of low salinity during larval development, transcript
384 amounts of the seven paralogs were quantified in larvae cultivated at 10 and 35 ppt from
385 3 until 25 dph. No significant differences in metamorphic index or survival
386 (63.3±10.1% and 52.5±5.4% for 10 and 35 ppt, respectively) were observed between
387 salinities at 25 dph. In contrast, a significantly higher dry weight was observed for
388 larvae cultivated at 10 ppt at the end of the experiment (25 dph; 1.9±0.3 and 1.4±0.1 mg
389 $larvae^{-1}$ for 10 and 35 ppt, respectively). Expression patterns of the seven NKA β
390 paralogs during this experiment are depicted in Fig. 5. *atp1b1a, atp1b1b, atp1b2a,*
391 *atp1b2b, atp1b3a, atp1b3b* showed significant differences during development but not
392 between salinities ($p>0.05$). These paralogous genes showed the highest mRNA levels
393 at 3 dph reducing progressively during development to remain stable at metamorphosis.
394 In contrast, *atp1b4* mRNA levels increased significantly with age exhibiting higher
395 transcript amounts in 18 dph larvae incubated at 10 ppt (2.5-fold higher than at 35 ppt;
396 $p<0.05$).
397

398 *3.4 Effect of a salinity shift on transcript levels of atp1b1a, atp1b1b, atp1b2a, atp1b2b,*

399 *atp1b3a, atp1b3b and atp1b4 in juvenile's gills*

400 As the seven NKA β paralogous genes had detectable mRNA levels in the gill,
401 we evaluated their transcriptional response after transferring soles from seawater (35
402 ppt) to 5 or 60 pp water (Fig. 6). A significant increase of *atp1b1b* mRNA levels was
403 observed in soles exposed at the highest salinity (60 ppt) compared to 5 and 35 ppt
404 (two-way ANOVA; Salinity: $F_{2,30}$=75.2, p<0.001; Timepoint: $F_{4,30}$=1.8, p=0.16;
405 salinity*timepoint interaction: $F_{8,30}$=2.6, p<0.05). Transcript levels at 60 ppt were 2.8-,
406 5.0-, 10.6-, 10.8- and 4.2-fold higher than at 35 ppt at 24h, 48h, 72h, 96h, and 168h,
407 respectively (p<0.05). Also, small but significant differences between salinities for
408 *atp1b1a* mRNA levels were detected (two-way ANOVA; salinity: $F_{2,30}$=4.1, p<0.05;
409 Timepoint: $F_{4,30}$=2.3, p=0.09; salinity*timepoint interaction: $F_{8,30}$=0.7, p=0.716).
410 ANOVA identified main differences at 24 h (2-fold higher at 60 ppt than at 35 ppt;
411 p<0.05).

412 For *atp1b3a* and *atp1b3b*, small but significant differences in mRNA abundance
413 between salinities and time were detected with a higher expression at 5 ppt than at 35
414 and 60 ppt (*atp1b3a*: two-way ANOVA; salinity: $F_{2,30}$=6.3, p<0.05; timepoint:
415 $F_{4,30}$=2.9, p<0.01; salinity*timepoint interaction: $F_{8,30}$=0.7, p=0.69; *atp1b3b*: two-way
416 ANOVA; salinity: $F_{2,30}$=4, p<0.05; timepoint: $F_{4,30}$=4.0, p<0.05; salinity*timepoint
417 interaction: $F_{8,30}$=1.3, p=0.26). In the case of *atp1b3a*, main differences were identified
418 at 5 ppt 24 h (2.5-fold higher than at 35 ppt; p<0.05) whereas for *atp1b3b*, main
419 increase was observed at 5 ppt 48 h (4.3-fold higher than at 35 ppt; p<0.05).

420 For *atp1b4*, significant differences in mRNA levels were detected only between
421 sampling times but not due to salinity (two-way ANOVA; Salinity: $F_{2,30}$=2.4, p=0.11;
422 Timepoint: $F_{4,30}$=5.1, p<0.01; salinity*timepoint interaction: $F_{8,30}$=0.8, p=0.57).

Moreover, no significant differences in *atp1b2a* or *atp1b2b* transcript abundance were found at any time point or salinity condition (Fig. 6).

The *atp1b1a* and *atp1b1b* mRNA amounts were also evaluated in intestine and kidney due their high steady-state relative levels in these organs (Fig. 3), not detecting significant changes at any time point due to salinity (data not shown).

3.5 Effect of salinity on atp1b1b gene expression in newly hatched larvae and localization by whole-mount ISH (WISH).

As *atp1b1b* was mainly expressed in osmoregulatory organs, we selected this paralogous gene for further WISH characterization and qPCR analysis in newly hatched larvae incubated at 10 and 35 ppt. No differences in mRNA abundance between salinities were found ($p>0.05$; Fig. 7). Also, a small expression peak at 3 dph (mouth opening) was observed.

WISH analysis at 1 dph showed that *atp1b1b* mRNAs were mainly detected in gut and pronephric tubule although expression was also detected in gill, otic vesicle, and developing chordacentrum of the notochordal sheath (Fig. 8). WISH signal in gut tended to decrease between 1 and 3 dph in pronephric tubule and gut while expression appeared in otic vesicle starting at 2 dph. No differences between salinities were observed (data not shown).

4. Discussion

Membrane-spanning NKA β subunit plays a key role as chaperone assessing the correct folding and delivery of NKA α subunit to the plasma membrane as well as modulating NKA cation affinities and K^+ occlusion (Lingrel and Kuntzweiler, 1994; Blanco and Mercer, 1998). In this work, seven cDNA sequences encoding NKA β subunits (*atp1b1a*, *atp1b1b*, *atp1b2a*, *atp1b2b*, *atp1b3a*, *atp1b3b* and *atpa1b4*) have been characterized for the first time in the euryhaline teleost fish *S. senegalensis*. The seven paralogs exhibited a typical domain organization for P-type NKA β subunits with a short ICD, a single α-helice (TMD) and a long ECD. Moreover, conserved motifs and residues were identified including: a) three tyrosine residues responsible of the ectodomain and transmembrane interactions between α and β subunits and critical for the cation pumping and ion affinity of the holoenzyme (Geering, 2001; Hasler et al., 2001; Durr et al., 2009; Shinoda et al., 2009); b) six conserved cysteine residues involved in the formation of ECD disulfide bonds required for the proper assembly and trafficking of the NKA heterodimer (Noguchi et al., 1994; Kimura et al., 2002; Laughery et al., 2003); c) the conserved YYPYY motif that interacts with the SFGQ motif and other residues of α subunit to modulate cation transport (Geering et al., 1993; Shinoda et al., 2009); d) the TMD LI*XX*G*XXX*G*XXX*G motif associated to subunit oligomerization and formation of α-β-β-α complexes (Hasler et al., 2001); e) an amino acid insertion region (with a species-specific sequence) typical of β1 subunits and crucial for dimerization as well as formation and maintenance of epithelial junctions (Tokhtaeva et al., 2012b; Vagin et al., 2012). Furthermore, a variable number of potential N-glycosylation sites (from 2 to 5) were detected in the ECD at different locations, depending on the paralogous gene. This number of glycosylation sites is in

466 agreement with what is observed in mammals (Toyoshima et al., 2011). N-glycosylation
467 has been shown to play an important role in the initial folding of the oligomer (Beggah
468 et al., 1997), intercellular junctions, cell polarization and protease protection (Laughery
469 et al., 2003; Vagin et al., 2006; Tokhtaeva et al., 2011). Overall, the structural analysis
470 of the seven Senegalese sole NKA β paralogs suggests they are functional as they
471 contain all the necessary elements for proper folding, integration in the membrane,
472 stabilization of the holoenzyme and epithelial adherent function in the case of NKAβ1a
473 and NKAβ1b.

474 Percentages of peptide identities between sole NKA β paralogs were lower
475 (25.6-66.7%) than those reported for the set of α subunit paralogs (81.3-92.6%)
476 (Armesto et al., 2014). These low identity values for β subunits were also reported in
477 other fish species (Cutler et al., 2000; Rajarao et al., 2002) and seem to be associated to
478 structural and functional constraints imposing distinct evolution rates to α and β
479 subunits. Transmembrane α-helices of P-type ATPases are highly conserved and act as
480 key structures for reorganization within the plane of the plasma membrane during ion-
481 translocation (Bublitz et al., 2010). The high number of TMDs (10) as well as the high
482 degree of amino acid homology in several α subunit regions involved in ATP binding
483 impose a lower evolutionary rate than for β subunits with only 1 TMD and with no
484 ligand binding site (Blanco and Mercer, 1998; Oberai et al., 2009; Armesto et al., 2014).
485 In spite of these lower sequence identities, phylogenetic analysis depicted a tree
486 topology in which NKA β sequences were clearly arranged in four major clades,
487 referred to as β1, β2, β3 and β4. Moreover, the overall set of NKA β subunits in sole
488 included duplicate paralogous genes encoding for β1 (*atp1b1a* and *atp1b1b*), β2
489 (*atp1b2a* and *atp1b2b*) and β3 (*atp1b3a* and *atp1b3b*), probably as a result of the teleost

490 specific whole-genome duplication that occurred during the fish evolutionary lineage
491 about 350 million years ago (Meyer and Van de Peer, 2005; Volff, 2005). A search of
492 NKA β sequences across fish species at the Ensembl database and further phylogenetic
493 analysis confirmed that they clustered correctly across Actinopterygii and Sarcoptergyii
494 species as previously reported (Rajarao et al., 2001; Rajarao et al., 2002). This retention
495 of a high number of β subunits could be associated to subfunctionalization or
496 neofunctionalization processes as occurs with *atp1b4* (also known as βm) that during
497 evolution has modified its function acting as a co-regulator of gene expression during
498 muscle development through TGF-β signaling in mammals and losing its capacity to
499 associate with the α catalytic subunit (Pestov et al., 2007). If we consider the set of
500 NKA β subunits (7) described in this work (although we cannot exclude the existence of
501 other additional paralogous genes) and the five paralogous genes for the α subunits
502 previously identified in sole (Armesto et al., 2014), at least 35 possible different
503 α/β combinations could occur in this species In zebrafish, up to 54 putative
504 combinations were predicted (that might be even higher if *atp1b4* paralog is considered)
505 although only 14 were confirmed according to their spatial distribution and expression
506 patterns (Blasiole et al., 2002; Canfield et al., 2002; Rajarao et al., 2002; Cheng et al.,
507 2003). This high number of paralogs encoding for α and β NKA subunits could
508 represent an adaptive mechanism for spatial-specialization to fine-tune osmotic
509 regulation under fluctuating ionic conditions.

510 The seven β subunit paralogous genes showed distinct expression profiles in
511 organs of juvenile soles (Fig. 3 and 4). Although mRNA transcripts for all paralogous
512 genes could be detected in brain, the *atp1b2a*, *atp1b2b*, *atp1b3a*, *atp1b3b* and *atp1b4*
513 revealed as highly brain-expressed isoforms. In contrast, *atp1b1b* showed the highest

514 mRNA levels in osmoregulatory organs (gill, intestine and kidney) and *atp1b1a* was
515 ubiquitously detected in the tissues examined (with the lowest mRNA levels in
516 intestine). These expression patterns were confirmed by a further analysis of brain
517 regions that clearly localized the highly brain-expressed isoforms (β2-, β3- and β4-
518 types) in regions rich in neurons and glia (hypothalamus, optic tectum and
519 telencephalon) while the more ubiquitous β1-type subunits were expressed in both brain
520 and pituitary. These data are in agreement with previous studies which showed a high
521 expression of β2 and β3 isoforms in nervous tissues in fish and tetrapods with different
522 temporal and spatial distribution (Appel et al., 1996; Cutler et al., 1997a; Canfield et al.,
523 2002; Rajarao et al., 2002; Man, 2012). This is also the case for paralog β4 in fish
524 (Pestov et al., 2007). Some specific roles of these specific NKA subunits in neurons,
525 glia cells and astrocytes were associated with signal transduction and membrane
526 polarization (Lees, 1991; Man, 2012), neuronal activity, glutamate uptake and energy
527 metabolism in astrocytes (Cholet et al., 2002; Rose et al., 2009; Tokhtaeva et al., 2012a)
528 and as adhesion molecule in the brain, capable of promoting neurite growth *in vitro*
529 (Muller-Husmann et al., 1993; Man, 2012). Interestingly, kinetic characteristics of α/β
530 NKA heterodimers involving β2 isoforms exhibit a lower K^+ affinity facilitating the
531 external K^+ clearance after membrane depolarization (Crambert et al., 2000). In
532 contrast, β1-type subunits are more ubiquitously expressed showing distinct expression
533 patterns between paralogs in tissues (Cutler et al., 1995; Cutler et al., 2000). They have
534 been mainly related to osmoregulation, hydromineral balance, signal transduction and
535 modulation of intercellular adhesion in epithelia (Cutler et al., 1995; Cutler et al., 2000;
536 Tokhtaeva et al., 2011).

537 Larvae cultivated at low salinity exhibited an optimal growth as previously

538 described (Salas-Leiton et al., 2012) indicating that once they have opened the mouth
539 larvae can successfully activate homeostatic mechanisms to adapt to hypoosmotic
540 conditions. At transcriptional level, the NKA β sole paralogs showed different
541 expression profiles during larval development (Fig. 5). The nervous-specific paralogs
542 *atp1b2a*, *atp1b2b* *atp1b3a* and *atp1b3b* decreased mRNA abundance during
543 development showing a expression profile similar to other genes also expressed in brain
544 or pituitary such as *atp1a3a* and *atp1a3b*, thyroid stimulating hormone β subunit (*tshb*)
545 or thyrotropin-releasing hormone (*trh*) (Manchado et al., 2008a; Iziga et al., 2010;
546 Ponce et al., 2010; Armesto et al., 2014). As mRNA levels were quantified in whole
547 larvae, this reduction during development could be explained, at least in part, by a
548 restricted expression pattern and progressively reduction of their contribution to the
549 total bulk of RNA in whole larvae. Moreover, the *atp1b1a* and *atp1b1b* paralogs,
550 expressed mainly in osmoregulatory tissues, showed similar expression profiles with
551 higher mRNA levels at 3 dph (Fig 5 and Fig. 7). These higher mRNA levels coincide
552 with the increase of α-type paralog *atp1a1a* mRNA abundance (Armesto et al., 2014)
553 probably related with ionocytes maturation in young larvae. Intriguingly, expression of
554 *atp1b4* increased at the final of metamorphosis in spite of it was mainly detected in the
555 brain of juvenile soles. This suggests that this gene was differently regulated compared
556 to the other highly nervous-expressed β2 and β3 paralogs. Moreover, *atp1b4* mRNA
557 levels were significantly higher in larvae cultivated at low salinity (10 ppt) than at 35
558 ppt at 18 dph. Developmental-specific responses to environmental salinities were
559 reported in eel (yellow or silver) for a β1 isoform (b233) (Cutler et al., 2000). As
560 NKA β4 subunit has undergone a neofunctionalization process in tetrapods with a
561 change in their tissue specificity (Pestov et al., 1999; Pestov et al., 2007), we cannot
562 exclude that the differences observed could be associated to temporal differences in the

563 ontogeny of a specific tissue. Further research will be necessary to elucidate exactly the
564 role of this β isoform in osmoregulation during development as well as its distribution
565 pattern in a wider set of tissues that could allow for a better understanding of the
566 expression profiles observed.

567 As the *atp1b1b* paralog showed a transcriptional activation in gill after the exposure
568 to a hypersalinity environment in a similar way to the α-paralog *atp1a1a* (Armesto et
569 al., 2014), this gene was further characterized by WISH. The *atp1b1b* transcripts were
570 mainly localized in osmoregulatory organs including pronephros tubule, gut and gills as
571 well as in the otic vesicle and in presumptive chordacentrum. Moreover, WISH signal in
572 the gut decreased from 1 to 3 dph whereas it increased in the gill. This expression
573 pattern is quite similar to that observed for *atp1a1a* (Armesto et al., 2014), which
574 strongly suggests that α1a/β1b combination is the active isozyme in these tissues in
575 larvae. In zebrafish embryos, β1a was the only NKA β isoform detectable in pronephros
576 but also expressed in lens, ear, olfactory placode and heart and β1b was mainly detected
577 in mucous cells (Canfield et al., 2002). Nevertheless, in gill ionocytes β1b isoform
578 combines with at least three different α1 subunits in an ionocyte-specific way to
579 regulate specifically the uptake of Na^+, Ca^{2+}, and Cl^- (Liao et al., 2009). These data
580 confirm the important role of β1b as an osmoregulatory isoform and the existence of
581 subfunctionalization during evolution modulated by the number and subtype of α and β
582 subunits duplicates retained in each species. Strikingly, *atp1b1b* was detected in
583 presumptive chordacentrum as observed for *atp1a1a* (Armesto et al., 2014).
584 Chondrocytes extracellular matrix has an unusual and variable ionic charge and osmotic
585 pressure and several NKA isozyme isoforms have been associated to the ionic transport
586 mechanism necessary to accomplish chondrocytes transmembrane constant fluxes

587 (Mobasheri et al., 1998; Shakibaei and Mobasheri, 2003; Mobasheri et al., 2012).
588 Extracellular matrix is not only a mechanical structure in articular cartilage and its
589 protein composition is also essential for chondrocyte differentiation (von der Mark et
590 al., 1977; Hirsch et al., 1997). Thus, this novel localization of NKA β isoforms,
591 similarly to *atp1a1a* (Armesto et al., 2014), strengthens the functional role of NKA in
592 fish notochordal sheath and vertebrae formation.

593 Senegalese sole adaptive response to a salinity change occurs in two phases, an
594 immediate adjustment period (until 7 days post-transfer) followed by a chronic
595 regulatory period when plasma osmolality becomes stable (Arjona et al., 2007). NKA
596 activity in the gill increases significantly in the second period (from 7 to 17 days) after
597 transferring soles to high salinity (55 ppt) (Arjona et al., 2007). Previous results on
598 *atp1a1a* gene expression showed that transcription of this paralog is also activated in
599 the gill after transferring soles to high salinity (60 ppt) (Armesto et al., 2014). In this
600 work, we demonstrate that *atp1b1b* also increases its mRNA amounts in gills from 48 h
601 to 7 d after transfer soles to 60 ppt. All these results indicate that Senegalese sole
602 response to hypersalinity is regulated at transcriptional levels and that α1a/β1b could be
603 the major isoenzyme involved in the chronic adaptation to high environmental ion
604 levels. Nevertheless, *atp1b1a* transcripts also increased slightly at 60 ppt although
605 response was weaker and earlier (at 24 h) than for *atp1b1b*. These temporal differences
606 in β1 paralogous gene activation could facilitate an earlier but sustained response to
607 maintain hydromineral balance in the adjustment period. Previous studies also reported
608 an increase of mRNA abundance of NKA β1 subunits in eels after transferring from
609 freshwater to seawater and a hypersaline environment (200% seawater) (Cutler et al.,
610 1995; Cutler et al., 2000) and during smoltification in salmon (Seidelin et al., 2001;

611 Nilsen et al., 2007) confirming the role of β1 subunits to adapt to high salinity
612 acclimation. In contrast, *atp1b3a* and *atp1b3b* a transient transcription peak after
613 transferring to low salinity (5 ppt). Similar results were obtained for the
614 α subunit *atp1a3a* that also exhibited a small but significant increased of mRNA levels
615 at 5 ppt in gills (Armesto et al., 2014). Previous studies demonstrated a switch in the
616 expression patterns of α isoforms in response to salinity changes in the gill of trout
617 (Richards et al., 2003), salmon (Madsen et al., 2009) and tilapia (Tipsmark et al., 2011).
618 Nevertheless, expression results in tissues indicate that NKA α3a, β3a and β3b subunits
619 are detected mainly in nervous tissue (this study; Armesto et al., 2014). The close
620 relationship observed between ionocytes and nerve fibers for O_2 sensing and ion
621 regulation (Jonz and Nurse, 2006) suggests these isoforms can successfully combine in
622 gill in response to low salinity to trigger a regulatory signalling response to maintain
623 homeostasis.

624 In summary, in this study the sequence and main features of seven cDNAs encoding
625 NKA β isoforms in the Senegalese sole are reported. The high level of structural and
626 motif conservation indicated that these sole NKA β paralogous genes encode for
627 functional proteins. Phylogeny clustered the seven paralogous sole genes into four main
628 clades (β1, β2, β3 and β4) with the orthologues from other fish. Expression profiles
629 showed that β2, β3 and β4 were mainly expressed in neuronal tissues while β1 were
630 more ubiquitous, although β1b was mainly detected in osmoregulatory organs. During
631 development, they exhibited different expression profiles but only *atp1b4* was
632 upregulated by low salinity during metamorphosis suggesting a osmoregulatory role
633 during development. WISH identified *atp1b1b* mainly localized in osmoregulatory
634 organs and in the chordacentrum of developing sole (3 dph). Moreover, *atp1b1b*, and

635 secondary *atp1b1a*, revealed as the main NKA β paralogs involved in hypersalinity
636 adaptation in gills while *atp1b3a* and *atp1b3b* paralogs could be involved in the
637 response to low salinity.

638

639 **Acknowledgements**

640 This study has been funded by project AQUAGENET (SOE2/P1/E287) program
641 INTERREG IVB SUDOE (ERDF/FEDER) and RTA2009-00066-00-00 from Instituto
642 Nacional de Investigación y tecnología Agraria y Alimentaria (INIA). PA is supported
643 by a PhD fellowship of IFAPA (Consejería de Agricultura y Pesca de la Junta de
644 Andalucía) and funded by the Operational Program of European Social Fund 2007-2013
645 of Andalucía, within the priority axis 3 (Expand and improve investment in human
646 capital) in 80%. We are grateful to Lucette Joassard for her assistance in WISH
647 analyses.

648

References

Abascal, F., Zardoya, R., Posada, D., 2005. ProtTest: selection of best-fit models of protein evolution. Bioinformatics 21, 2104-2105.

Antonicek, H., Schachner, M., 1988. The adhesion molecule on glia (AMOG) incorporated into lipid vesicles binds to subpopulations of neurons. J. Neurosci. 8, 2961-2966.

Appel, C., Gloor, S., Schmalzing, G., Schachner, M., Bernhardt, R.R., 1996. Expression of a Na,K-ATPase β3 subunit during development of the zebrafish central nervous system. J. Neurosci. Res. 46, 551-564.

Arjona, F.J., Vargas-Chacoff, L., Ruiz-Jarabo, I., Martin del Rio, M.P., Mancera, J.M., 2007. Osmoregulatory response of Senegalese sole (*Solea senegalensis*) to changes in environmental salinity. Comp. Biochem. Physiol. A Mol. Integr. Physiol. 148, 413-421.

Armesto, P., Campinho, M.A., Rodriguez-Rua, A., Cousin, X., Power, D.M., Manchado, M., Infante, C., 2014. Molecular characterization and transcriptional regulation of the Na^+/K^+ ATPase α subunit isoforms during development and salinity challenge in a teleost fish, the Senegalese sole (*Solea senegalensis*). Comp. Biochem. Physiol. B Biochem. Mol. Biol. 175, 23-38.

Beggah, A.T., Jaunin, P., Geering, K., 1997. Role of glycosylation and disulfide bond formation in the beta subunit in the folding and functional expression of Na,K-ATPase. J. Biol. Chem. 272, 10318-10326.

Bensimon-Brito, A., Cardeira, J., Cancela, M.L., Huysseune, A., Witten, P.E., 2012. Distinct patterns of notochord mineralization in zebrafish coincide with the localization of Osteocalcin isoform 1 during early vertebral centra formation. BMC Dev. Biol. 12, 28.

673 Benzekri, H., Armesto, P., Cousin, X., Rovira, M., Crespo, D., Merlo, M.A., Mazurais,
674 D., Bautista, R., Guerrero-Fernandez, D., Fernandez-Pozo, N., Ponce, M., Infante, C.,
675 Zambonino, J.L., Nidelet, S., Gut, M., Rebordinos, L., Planas, J.V., Begout, M.L.,
676 Claros, M.G., Manchado, M., 2014. *De novo* assembly, characterization and functional
677 annotation of Senegalese sole (*Solea senegalensis*) and common sole (*Solea solea*)
678 transcriptomes: integration in a database and design of a microarray. BMC Genomics
679 15, 952.
680 Blanco, G., Sanchez, G., Mercer, R.W., 1995. Comparison of the enzymatic properties
681 of the Na,K-ATPase α3β1 and α3β2 isozymes. Biochemistry 34, 9897-9903.
682 Blanco, G., Mercer, R.W., 1998. Isozymes of the Na-K-ATPase: heterogeneity in
683 structure, diversity in function. Am. J. Physiol. 275, F633-650.
684 Blanco, G., 2005. Na,K-ATPase subunit heterogeneity as a mechanism for tissue-
685 specific ion regulation. Semin. Nephrol. 25, 292-303.
686 Blasiole, B., Canfield, V., Degrave, A., Thisse, C., Thisse, B., Rajarao, J., Levenson, R.,
687 2002. Cloning, mapping, and developmental expression of a sixth zebrafish Na,K-
688 ATPase α1 subunit gene (*atp1a1a*.5). Mech. Dev. 119 Suppl 1, S211-214.
689 Blasiole, B., Canfield, V.A., Vollrath, M.A., Huss, D., Mohideen, M.A., Dickman, J.D.,
690 Cheng, K.C., Fekete, D.M., Levenson, R., 2006. Separate Na,K-ATPase genes are
691 required for otolith formation and semicircular canal development in zebrafish. Dev.
692 Biol. 294, 148-160.
693 Bublitz, M., Poulsen, H., Morth, J.P., Nissen, P., 2010. In and out of the cation pumps:
694 P-type ATPase structure revisited. Curr. Opin. Struct. Biol. 20, 431-439.
695 Canfield, V.A., Loppin, B., Thisse, B., Thisse, C., Postlethwait, J.H., Mohideen, M.A.,
696 Rajarao, S.J., Levenson, R., 2002. Na,K-ATPase α and β subunit genes exhibit unique
697 expression patterns during zebrafish embryogenesis. Mech. Dev. 116, 51-59.

698 Cerda, J., Mercade, J., Lozano, J.J., Manchado, M., Tingaud-Sequeira, A., Astola, A.,
699 Infante, C., Halm, S., Vinas, J., Castellana, B., Asensio, E., Canavate, P., Martinez-
700 Rodriguez, G., Piferrer, F., Planas, J.V., Prat, F., Yufera, M., Durany, O., Subirada, F.,
701 Rosell, E., Maes, T., 2008. Genomic resources for a commercial flatfish, the Senegalese
702 sole (*Solea senegalensis*): EST sequencing, oligo microarray design, and development
703 of the Soleamold bioinformatic platform. BMC Genomics 9, 508.
704 Cheng, K.C., Levenson, R., Robishaw, J.D., 2003. Functional genomic dissection of
705 multimeric protein families in zebrafish. Dev. Dyn. 228, 555-567.
706 Cholet, N., Pellerin, L., Magistretti, P.J., Hamel, E., 2002. Similar perisynaptic glial
707 localization for the Na^+,K^+-ATPase α2 subunit and the glutamate transporters GLAST
708 and GLT-1 in the rat somatosensory cortex. Cereb. Cortex 12, 515-525.
709 Chow, D.C., Forte, J.G., 1995. Functional significance of the β-subunit for
710 heterodimeric P-type ATPases. J. Exp. Biol. 198, 1-17.
711 Crambert, G., Hasler, U., Beggah, A.T., Yu, C., Modyanov, N.N., Horisberger, J.D.,
712 Lelievre, L., Geering, K., 2000. Transport and pharmacological properties of nine
713 different human Na, K-ATPase isozymes. J. Biol. Chem. 275, 1976-1986.
714 Cutler, C.P., Sanders, I.L., Hazon, N., Cramb, G., 1995. Primary sequence, tissue
715 specificity and mRNA expression of the Na^+,K^+-ATPase β1 subunit in the European eel
716 (*Anguilla anguilla*). Fish Physiol. Biochem. 14, 423-429.
717 Cutler, C.P., Sanders, I.L., Cramb, G., 1997a. Isolation of six putative P-type ATPase β
718 subunit PCR fragments from the brain of the European eel (*Anguilla anguilla*). Ann. N.
719 Y. Acad. Sci. 834, 123-125.
720 Cutler, C.P., Sanders, I.L., Cramb, G., 1997b. Expression of Na^+,K^+-ATPase β subunit
721 isoforms in the European eel (*Anguilla anguilla*). Fish Physiol. Biochem. 17, 371-376.

722 Cutler, C.P., Brezillon, S., Bekir, S., Sanders, I.L., Hazon, N., Cramb, G., 2000.
723 Expression of a duplicate Na,K-ATPase β_1-isoform in the European eel (*Anguilla*
724 *anguilla*). Am. J. Physiol. Regul. Integr. Comp. Physiol. 279, R222-229.
725 Deane, E.E., Woo, N.Y., 2005. Cloning and characterization of sea bream Na^+-K^+-
726 ATPase α and β subunit genes: *In vitro* effects of hormones on transcriptional and
727 translational expression. Biochem. Biophys. Res. Commun. 331 1229-1238.
728 Durr, K.L., Tavraz, N.N., Dempski, R.E., Bamberg, E., Friedrich, T., 2009. Functional
729 significance of E_2 state stabilization by specific α/β -subunit interactions of Na,K- and
730 H,K-ATPase. J. Biol. Chem. 284, 3842-3854.
731 Felsenstein, J., 1989. PHYLIP - Phylogeny Inference Package (Version 3.2). Cladistics
732 5, 164-166.
733 Geering, K., 1991. The functional role of the β-subunit in the maturation and
734 intracellular transport of Na,K-ATPase. FEBS Lett. 285, 189-193.
735 Geering, K., Jaunin, P., Jaisser, F., Merillat, A.M., Horisberger, J.D., Mathews, P.M.,
736 Lemas, V., Fambrough, D.M., Rossier, B.C., 1993. Mutation of a conserved proline
737 residue in the β-subunit ectodomain prevents Na^+-K^+-ATPase oligomerization. Am. J.
738 Physiol. 265, C1169-1174.
739 Geering, K., Beggah, A., Good, P., Girardet, S., Roy, S., Schaer, D., Jaunin, P., 1996.
740 Oligomerization and maturation of Na,K-ATPase: Functional interaction of the
741 cytoplasmic NH_2 terminus of the β subunit with the α subunit. J. Cell Biol. 133, 1193-
742 1204.
743 Geering, K., 2001. The functional role of β subunits in oligomeric P-type ATPases. J.
744 Bioenerg. Biomembr. 33, 425-438.
745 Geering, K., 2008. Functional roles of Na,K-ATPase subunits. Curr. Opin. Nephrol.
746 Hypertens. 17, 526-532.

747 Gharbi, K., Ferguson, M.M., Danzmann, R.G., 2005. Characterization of Na, K-ATPase
748 genes in Atlantic salmon (*Salmo salar*) and comparative genomic organization with
749 rainbow trout (*Oncorhynchus mykiss*). Mol. Genet. Genomics 273, 474-483.
750 Gloor, S., Antonicek, H., Sweadner, K.J., Pagliusi, S., Frank, R., Moos, M., Schachner,
751 M., 1990. The adhesion molecule on glia (AMOG) is a homologue of the β subunit of
752 the Na,K-ATPase. J. Cell Biol. 110, 165-174.
753 Guindon, S., Dufayard, J.F., Lefort, V., Anisimova, M., Hordijk, W., Gascuel, O., 2010.
754 New algorithms and methods to estimate maximum-likelihood phylogenies: assessing
755 the performance of PhyML 3.0. Syst. Biol. 59, 307-321.
756 Hasler, U., Wang, X., Crambert, G., Beguin, P., Jaisser, F., Horisberger, J.D., Geering,
757 K., 1998. Role of β-subunit domains in the assembly, stable expression, intracellular
758 routing, and functional properties of Na,K-ATPase. J. Biol. Chem. 273, 30826-30835.
759 Hasler, U., Crambert, G., Horisberger, J.D., Geering, K., 2001. Structural and functional
760 features of the transmembrane domain of the Na,K-ATPase β subunit revealed by
761 tryptophan scanning. J. Biol. Chem. 276, 16356-16364.
762 Herrera, M., Aragão, C., Hachero, I., Ruiz-Jarabo, I., Vargas-Chacoff, L., Mancera,
763 J.M., Conceicão, L.E., 2012. Physiological short-term response to sudden salinity
764 change in the Senegalese sole (*Solea senegalensis*). Fish Physiol. Biochem. 38, 1741-
765 1751.
766 Hirsch, M.S., Lunsford, L.E., Trinkaus-Randall, V., Svoboda, K.K., 1997. Chondrocyte
767 survival and differentiation in situ are integrin mediated. Dev. Dyn. 210, 249-263.
768 Hofmann, K., Stoffel, W., 1993. TMBASE - A database of membrane spanning protein
769 segments. Biol. Chem. Hoppe-Seyler 374, 166.

770 Infante, C., Matsuoka, M.P., Asensio, E., Cañavate, J.P., Reith, M., Manchado, M.,
771 2008. Selection of housekeeping genes for gene expression studies in larvae from
772 flatfish using real-time PCR. BMC Mol. Biol. 9, 28.
773 Iziga, R., Ponce, M., Infante, C., Rebordinos, L., Cañavate, J.P., Manchado, M., 2010.
774 Molecular characterization and gene expression of thyrotropin-releasing hormone in
775 Senegalese sole (*Solea senegalensis*). Comp. Biochem. Physiol. B Biochem. Mol. Biol.
776 157, 167-174.
777 Jonz, M.G., Nurse, C.A., 2006. Epithelial mitochondria-rich cells and associated
778 innervation in adult and developing zebrafish. J. Comp. Neurol. 497, 817-832.
779 Kimura, T., Tabuchi, Y., Takeguchi, N., Asano, S., 2002. Mutational study on the roles
780 of disulfide bonds in the β-subunit of gastric H^+,K^+-ATPase. J. Biol. Chem. 277, 20671-
781 20677.
782 Laughery, M., Todd, M., Kaplan, J.H., 2004. Oligomerization of the Na,K-ATPase in
783 cell membranes. J. Biol. Chem. 279, 36339-36348.
784 Laughery, M.D., Todd, M.L., Kaplan, J.H., 2003. Mutational analysis of α-β subunit
785 interactions in the delivery of Na,K-ATPase heterodimers to the plasma membrane. J.
786 Biol. Chem. 278, 34794-34803.
787 Lees, G.J., 1991. Inhibition of sodium-potassium-ATPase: a potentially ubiquitous
788 mechanism contributing to central nervous system neuropathology. Brain Res. Rev. 16,
789 283-300.
790 Liao, B.K., Chen, R.D., Hwang, P.P., 2009. Expression regulation of Na^+-K^+-ATPase
791 α1-subunit subtypes in zebrafish gill ionocytes. Am. J. Physiol. Regul. Integr. Comp.
792 Physiol. 296, R1897-1906.
793 Lingrel, J.B., Kuntzweiler, T., 1994. Na^+,K^+-ATPase. J. Biol. Chem. 269, 19659-19662.

794 Linnertz, H., Urbanova, P., Obsil, T., Herman, P., Amler, E., Schoner, W., 1998.
795 Molecular distance measurements reveal an $(\alpha\beta)_2$ dimeric structure of Na^+/K^+-ATPase.
796 High affinity ATP binding site and K^+-activated phosphatase reside on different α-
797 subunits. J. Biol. Chem. 273, 28813-28821.
798 Livak, K.J., Schmittgen, T.D., 2001. Analysis of relative gene expression data using
799 real-time quantitative PCR and the $2^{-(\Delta\Delta Ct)}$ Method. Methods 25, 402-408.
800 Lutsenko, S., Kaplan, J.H., 1993. An essential role for the extracellular domain of the
801 Na,K-ATPase β-subunit in cation occlusion. Biochemistry 32, 6737-6743.
802 Madsen, S.S., Kiilerich, P., Tipsmark, C.K., 2009. Multiplicity of expression of Na^+,K^+-
803 ATPase α-subunit isoforms in the gill of Atlantic salmon (*Salmo salar*): cellular
804 localisation and absolute quantification in response to salinity change. J. Exp. Biol. 212,
805 78-88.
806 Man, H.Y., 2012. The sodium pump: novel functions in the brain. Biochem. Anal.
807 Biochem. 1, e116.
808 Manchado, M., Infante, C., Asensio, E., Cañavate, J.P., 2007. Differential gene
809 expression and dependence on thyroid hormones of two glyceraldehyde-3-phosphate
810 dehydrogenases in the flatfish Senegalese sole (*Solea senegalensis* Kaup). Gene 400, 1-
811 8.
812 Manchado, M., Infante, C., Asensio, E., Planas, J.V., Cañavate, J.P., 2008a. Thyroid
813 hormones down-regulate thyrotropin β subunit and thyroglobulin during metamorphosis
814 in the flatfish Senegalese sole (*Solea senegalensis* Kaup). Gen. Comp. Endocrinol. 155,
815 447-455.
816 Manchado, M., Salas-Leiton, E., Infante, C., Ponce, M., Asensio, E., Crespo, A., Zuasti,
817 E., Cañavate, J.P., 2008b. Molecular characterization, gene expression and

818 transcriptional regulation of cytosolic *HSP90* genes in the flatfish Senegalese sole
819 (*Solea senegalensis* Kaup). Gene 416, 77-84.
820 Manchado, M., Infante, C., Rebordinos, L., Cañavate, J.P., 2009. Molecular
821 characterization, gene expression and transcriptional regulation of thyroid hormone
822 receptors in Senegalese sole. Gen. Comp. Endocrinol. 160, 139-147.
823 Martin-Vasallo, P., Dackowski, W., Emanuel, J.R., Levenson, R., 1989. Identification
824 of a putative isoform of the Na,K-ATPase β subunit. Primary structure and tissue-
825 specific expression. J. Biol. Chem. 264, 4613-4618.
826 Martínez-Velasco, C., Forja, J.M., Gómez-Parra, A., 1999. Hydrochemistry
827 characterisation of protected marine ecosystems in Cadiz. Bol. Inst. Esp. Oceanogr. 15,
828 451-456.
829 McCormick, S.D., Regish, A.M., Christensen, A.K., 2009. Distinct freshwater and
830 seawater isoforms of Na^+/K^+-ATPase in gill chloride cells of Atlantic salmon. J. Exp.
831 Biol. 212, 3994-4001.
832 Meyer, A., Van de Peer, Y., 2005. From 2R to 3R: evidence for a fish-specific genome
833 duplication (FSGD). Bioessays 27, 937-945.
834 Mobasheri, A., Mobasheri, R., Francis, M.J., Trujillo, E., Alvarez de la Rosa, D.,
835 Martin-Vasallo, P., 1998. Ion transport in chondrocytes: membrane transporters
836 involved in intracellular ion homeostasis and the regulation of cell volume, free [Ca^{2+}]
837 and pH. Histol. Histopathol. 13, 893-910.
838 Mobasheri, A., Avila, J., Cozar-Castellano, I., Brownleader, M.D., Trevan, M., Francis,
839 M.J., Lamb, J.F., Martin-Vasallo, P., 2000. Na^+,K^+-ATPase isozyme diversity;
840 comparative biochemistry and physiological implications of novel functional
841 interactions. Biosci. Rep. 20, 51-91.

842 Mobasheri, A., Trujillo, E., Arteaga, M.F., Martin-Vasallo, P., 2012. Na^+, K^+-ATPase
843 subunit composition in a human chondrocyte cell line; Evidence for the Presence of α1,
844 α3, β1, β2 and β3 Isoforms. Int. J. Mol. Sci. 13, 5019-5034.
845 Muller-Husmann, G., Gloor, S., Schachner, M., 1993. Functional characterization of β
846 isoforms of murine Na,K-ATPase. The adhesion molecule on glia (AMOG/β2), but not
847 β1, promotes neurite outgrowth. J. Biol. Chem. 268, 26260-26267.
848 Nilsen, T.O., Ebbesson, L.O., Madsen, S.S., McCormick, S.D., Andersson, E.,
849 Bjornsson, B.T., Prunet, P., Stefansson, S.O., 2007. Differential expression of gill
850 Na^+,K^+-ATPase α- and β-subunits, Na^+,K^+,$2Cl^-$ cotransporter and CFTR anion channel
851 in juvenile anadromous and landlocked Atlantic salmon *Salmo salar*. J. Exp. Biol. 210,
852 2885-2896.
853 Noguchi, S., Mutoh, Y., Kawamura, M., 1994. The functional roles of disulfide bonds
854 in the β-subunit of (Na,K)ATPase as studied by site-directed mutagenesis. FEBS Lett.
855 341, 233-238.
856 Oberai, A., Joh, N.H., Pettit, F.K., Bowie, J.U., 2009. Structural imperatives impose
857 diverse evolutionary constraints on helical membrane proteins. Proc. Natl. Acad. Sci.
858 USA 106, 17747-17750.
859 Page, R.D.M., 1996. TREEVIEW: An application to display phylogenetic trees on
860 personal computers. Comp. Appl. Biosci. 12, 357-358.
861 Pagni, M., Ioannidis, V., Cerutti, L., Zahn-Zabal, M., Jongeneel, C.V., Hau, J., Martin,
862 O., Kuznetsov, D., Falquet, L., 2007. MyHits: improvements to an interactive resource
863 for analyzing protein sequences. Nucleic Acids Res. 35, W433-437.
864 Pestov, N.B., Adams, G., Shakhparonov, M.I., Modyanov, N.N., 1999. Identification of
865 a novel gene of the X,K-ATPase β-subunit family that is predominantly expressed in
866 skeletal and heart muscles. FEBS Lett. 456, 243-248.

867 Pestov, N.B., Ahmad, N., Korneenko, T.V., Zhao, H., Radkov, R., Schaer, D., Roy, S.,
868 Bibert, S., Geering, K., Modyanov, N.N., 2007. Evolution of Na,K-ATPase βm-subunit
869 into a coregulator of transcription in placental mammals. Proc. Natl. Acad. Sci. USA
870 104, 11215-11220.
871 Ponce, M., Infante, C., Manchado, M., 2010. Molecular characterization and gene
872 expression of thyrotropin receptor (TSHR) and a truncated TSHR-like in *Senegalese*
873 *sole*. Gen. Comp. Endocrinol. 168, 431-439.
874 Rajarao, J.R., Canfield, V.A., Loppin, B., Thisse, B., Thisse, C., Yan, Y.L.,
875 Postlethwait, J.H., Levenson, R., 2002. Two Na,K-ATPase β2 subunit isoforms are
876 differentially expressed within the central nervous system and sensory organs during
877 zebrafish embryogenesis. Dev. Dyn. 223, 254-261.
878 Rajarao, S.J., Canfield, V.A., Mohideen, M.A., Yan, Y.L., Postlethwait, J.H., Cheng,
879 K.C., Levenson, R., 2001. The repertoire of Na,K-ATPase α and β subunit genes
880 expressed in the zebrafish, *Danio rerio*. Genome Res. 11, 1211-1220.
881 Rajasekaran, S.A., Palmer, L.G., Moon, S.Y., Peralta Soler, A., Apodaca, G.L., Harper,
882 J.F., Zheng, Y., Rajasekaran, A.K., 2001a. Na,K-ATPase activity is required for
883 formation of tight junctions, desmosomes, and induction of polarity in epithelial cells.
884 Mol. Biol. Cell. 12, 3717-3732.
885 Rajasekaran, S.A., Palmer, L.G., Quan, K., Harper, J.F., Ball, W.J., Jr., Bander, N.H.,
886 Peralta Soler, A., Rajasekaran, A.K., 2001b. Na,K-ATPase β subunit is required for
887 epithelial polarization, suppression of invasion, and cell motility. Mol. Biol. Cell 12,
888 279-295.
889 Richards, J.G., Semple, J.W., Bystriansky, J.S., Schulte, P.M., 2003. Na+/K+-ATPase
890 α-isoform switching in gills of rainbow trout (*Oncorhynchus mykiss*) during salinity
891 transfer. J. Exp. Biol. 206, 4475-4486.

892 Rose, E.M., Koo, J.C., Antflick, J.E., Ahmed, S.M., Angers, S., Hampson, D.R., 2009.
893 Glutamate transporter coupling to Na,K-ATPase. J. Neurosci. 29, 8143-8155.
894 Salas-Leiton, E., Rodriguez-Rua, A., Asensio, E., Infante, C., Manchado, M.,
895 Fernandez-Diaz, C., Cañavate, J.P., 2012. Effect of salinity on egg hatching, yolk sac
896 absorption and larval rearing of Senegalese sole (*Solea senegalensis* Kaup 1858). Rev.
897 Aquaculture 4, 49-58.
898 Seidelin, M., Madsen, S.S., Cutler, C.P., Cramb, G., 2001. Expression of gill vacuolar-
899 type H^+-ATPase B subunit, and Na^+, K^+-ATPase α_1 and β_1 subunit messenger RNAs in
900 smolting *Salmo salar*. Zool. Sci. 18, 315-324.
901 Shakibaei, M., Mobasheri, A., 2003. β1-integrins co-localize with Na, K-ATPase,
902 epithelial sodium channels (ENaC) and voltage activated calcium channels (VACC) in
903 mechanoreceptor complexes of mouse limb-bud chondrocytes. Histol. Histopathol. 18,
904 343-351.
905 Shinoda, T., Ogawa, H., Cornelius, F., Toyoshima, C., 2009. Crystal structure of the
906 sodium-potassium pump at 2.4 Å resolution. Nature 459, 446-450.
907 Shyjan, A.W., Cena, V., Klein, D.C., Levenson, R., 1990. Differential expression and
908 enzymatic properties of the Na^+,K^+-ATPase α3 isoenzyme in rat pineal glands. Proc.
909 Natl. Acad. Sci. USA 87, 1178-1182.
910 Sweadner, K.J., 1985. Enzymatic properties of separated isozymes of the Na,K-ATPase.
911 Substrate affinities, kinetic cooperativity, and ion transport stoichiometry. J. Biol.
912 Chem. 260, 11508-11513.
913 Taniguchi, K., Kaya, S., Abe, K., Mardh, S., 2001. The oligomeric nature of Na/K-
914 transport ATPase. J. Biochem. 129, 335-342.
915 Thisse, C., Thisse, B., 2008. High-resolution in situ hybridization to whole-mount
916 zebrafish embryos. Nat. Protoc. 3, 59-69.

Tipsmark, C.K., Breves, J.P., Seale, A.P., Lerner, D.T., Hirano, T., Grau, E.G., 2011. Switching of Na^+, K^+-ATPase isoforms by salinity and prolactin in the gill of a cichlid fish. J. Endocrinol. 209, 237-244.

Tokhtaeva, E., Sachs, G., Souda, P., Bassilian, S., Whitelegge, J.P., Shoshani, L., Vagin, O., 2011. Epithelial junctions depend on intercellular trans-interactions between the Na,K-ATPase β_1 subunits. J. Biol. Chem. 286, 25801-25812.

Tokhtaeva, E., Clifford, R.J., Kaplan, J.H., Sachs, G., Vagin, O., 2012a. Subunit isoform selectivity in assembly of Na,K-ATPase α-β heterodimers. J. Biol. Chem. 287, 26115-26125.

Tokhtaeva, E., Sachs, G., Sun, H., Dada, L.A., Sznajder, J.I., Vagin, O., 2012b. Identification of the amino acid region involved in the intercellular interaction between the β1 subunits of Na^+/K^+ -ATPase. J. Cell Sci. 125, 1605-1616.

Tovar, A., Moreno, C., Mánuel-Vez, M.P., Garcia-Vargas, M., 2000. Environmental impacts of intensive aquaculture in marine waters. Wat. Res. 34, 334-342.

Toyoshima, C., Kanai, R., Cornelius, F., 2011. First crystal structures of Na^+,K^+-ATPase: new light on the oldest ion pump. Structure 19, 1732-1738.

Vagin, O., Tokhtaeva, E., Sachs, G., 2006. The role of the β1 subunit of the Na,K-ATPase and its glycosylation in cell-cell adhesion. J. Biol. Chem. 281, 39573-39587.

Vagin, O., Dada, L.A., Tokhtaeva, E., Sachs, G., 2012. The Na-K-ATPase $\alpha_1\beta_1$ heterodimer as a cell adhesion molecule in epithelia. Am. J. Physiol. Cell Physiol. 302, C1271-1281.

Vandesompele, J., De Preter, K., Pattyn, F., Poppe, B., Van Roy, N., De Paepe, A., Speleman, F., 2002. Accurate normalization of real-time quantitative RT-PCR data by geometric averaging of multiple internal control genes. Genome Biol. 3, research0034.

941 Volff, J.N., 2005. Genome evolution and biodiversity in teleost fish. Heredity (Edinb)
942 94, 280-294.
943 von der Mark, K., Gauss, V., von der Mark, H., Muller, P., 1977. Relationship between
944 cell shape and type of collagen synthesised as chondrocytes lose their cartilage
945 phenotype in culture. Nature 267, 531-532.
946
947

Figure captions

Figure 1

Comparison of Senegalese sole NKA β proteins. Dots represent identity with NKA β1a, and dashes represent indels that allow optimal alignment. The predicted intracellular domain (ICD), transmembrane domain (TMD) and extracellular domain (ECD) are shaded in yellow, blue and purple. Potential N-Glycosylation sites and motifs are highlighted in dark and light pink respectively. Conserved motifs and sequences are boxed from 1 to 6. Conserved Tyrosines interacting with NKA α domains are marked with asterisks. Six cysteine residues involved in 3 conserved disulfide bonds are marked with arrows.

Figure 2

Phylogenetic relationships among the predicted sequence of Senegalese sole NKA β subunit paralogs and the corresponding deduced amino acid sequences from other vertebrates (see Additional file 1) using the Maximum Likelihood method. *Ciona intestinalis* NKA β subunit was used as outgroup to root tree. Only bootstrap values higher than 50% are indicated on each branch. The scale for branch length (0.1 substitutions/site) is shown below the tree. Apl: *Anas platyrhynchos*; Aca*: Anolis carolinensi*; Ame*: Astyanax mexicanus*; Bta*: Bos Taurus*; Cfa*: Canis lupus familiaris*; Cin*: Ciona intestinalis*; Cca: *Cyprinus carpio*; Dre*: Danio rerio*; Fca*: Felis catus,* Fal*: Ficedula albicollis,* Gga*: Gallus gallus*; Gac*: Gasterosteus aculeatus*; Ggo: *Gorilla gorilla gorilla*; Hsa: *Homo sapiens*; Lch: *Latimeria chalumnae*; Loc*: Lepisosteus*

oculatus; Laf: *Loxodonta africana*, Mga*: Meleagris gallopavo*; Mmu*: Mus musculus*, Oma*: Oncorhynchus masou*; Oni*: Oreochromis niloticus;* Ola*: Oryzias latipes*; Ptr*: Pan troglodytes;* Psi*: Pelodiscus sinensis*; Rno: *Rattus norvegicus;* Rsa: *Rhabdosargus sarba*; Sse*: Solea senegalensis*, Tru*: Takifugu rubripes;* Tni*: Tetraodon nigroviridis*, Xtr*: Xenopus tropicalis*; Xma*: Xiphophorus maculatus.*

Figure 3

Relative expression levels of NKA β genes in different tissues of Senegalese sole juveniles. Expression values were normalized to those of 18S rRNA. Data were expressed as the mean fold change (mean ± SEM, n = 3) from the calibrator group (spleen). Different letters denote statistically significant differences among tissues ($p < 0.05$) as determined with the Kruskal-Wallis test (non-parametric one-way ANOVA) followed by Fisher's Least Significant Difference (LSD) test. Sp: spleen; L: liver; I: intestine; B: brain; K: kidney; G: gills; Ht: heart; M: muscle; Sk: skin.

Figure 4

Relative expression levels of NKA β genes in different brain sections of Senegalese sole juveniles. Expression values were normalized to those of ubiquitin (*ub52*) Data were expressed as the mean fold change (mean ± SEM, n = 3) from the calibrator group (Pituitary). Different letters denote statistically significant differences among sections ($p < 0.05$) as determined with the Kruskal-Wallis test (non-parametric one-way ANOVA) followed by Fisher's Least Significant Difference (LSD) test. Pit: pituitary; Hth: hypothalamus; OT: optic tectum; Tel: Telencephalon.

Figure 5

Relative expression levels of NKA β genes in larvae incubated at 10 and 35 ppt. Expression values were normalized to those of the geometric mean between *ub52* and *gapdh2*. Data were expressed as the mean fold change (mean ± SEM, n = 3) from the calibrator group (10 ppt 3 dph, not represented). Significant differences in the relative expression levels by time or salinity were tested using a two-way ANOVA (p<0.05). Lowercase letters denote significant differences between sampling times and the asterisks significant differences between salinities at a specific time.

Figure 6

Transcript abundance of NKA β genes after salinity transfer (5, 35 and 60 ppt) in the gills of Senegalese sole juveniles. Expression values were normalized to those of *ub52*. Data were expressed as the mean fold change (mean ± SEM, n = 3 at 72 h, 96 h and 7 d) from the calibrator group (35 ppt 24 h). Significant differences in the relative expression levels by time or salinity were tested using a two-way ANOVA (p<0.05). Lowercase letters denote significant differences between sampling times and uppercase letter between salinities at a specific time.

Figure 7

Relative expression levels of *atp1b1b* in newly hatched larvae incubated at 10 and 35 ppt. Expression values were normalized to those of *gapdh2*. Data were expressed as the mean fold change (mean ± SEM, n = 3) from the calibrator group (10 ppt 1 dph). Significant differences in the relative expression levels by time or salinity were tested using a two-way ANOVA (p<0.05). Lowercase letters denote significant differences between days.

Figure 8

Whole mount analysis of *atp1b1b* in newly hatched sole larvae. Whole larvae in lateral and ventral views are shown (upper panel). A riboprobe from the sense strand was used as a control in 1 and 3 dph larvae (lower panel). (pt) pronephric tubule, (ch) chondracentrum, (g) gills, (ag) anterior gut, (pg) posterior gut, (ov) otic vesicule.

Figure 1

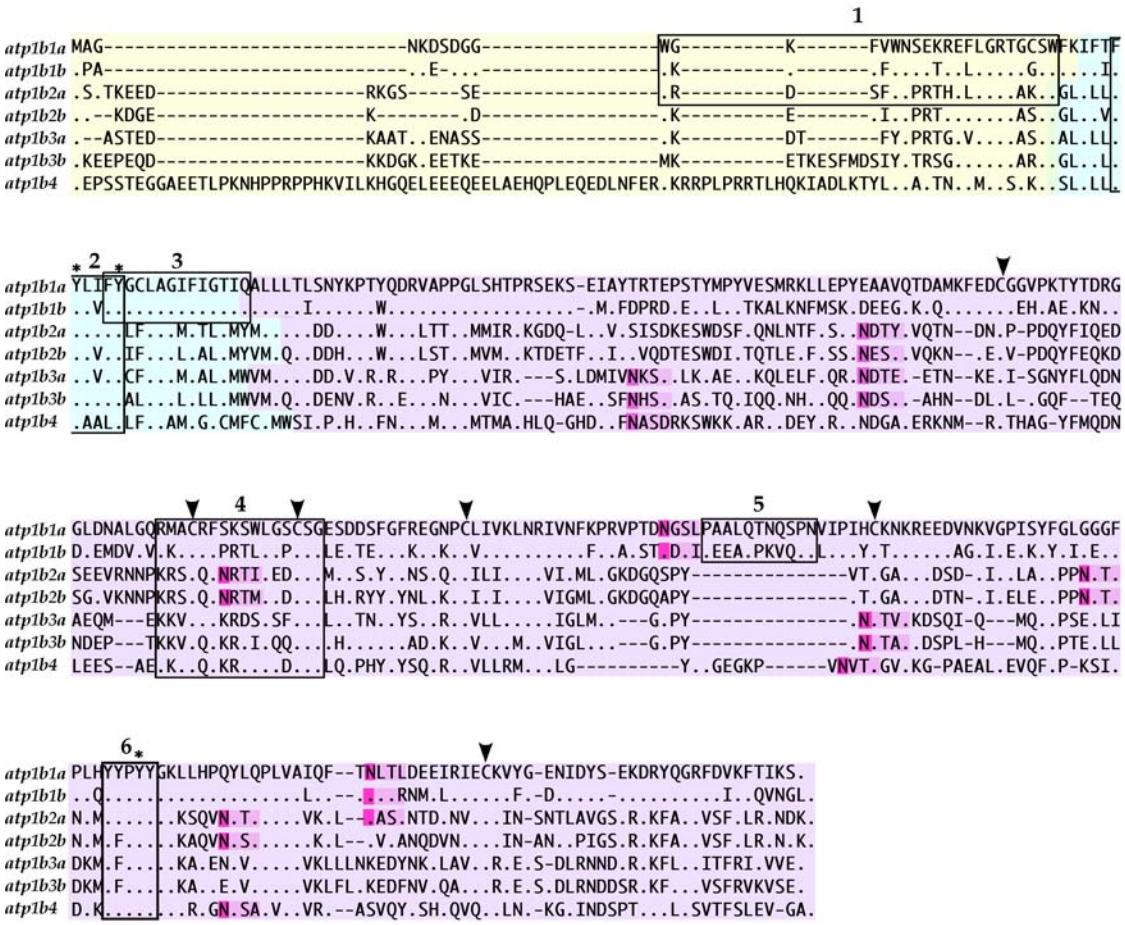
1
2
3
4
5
6
atp1b1a MAG----------NKDSDGG----------WG----------K-------FVWNSEKREFLGRTGCSWFKIFTF
atp1b1b .PA----------..E-...----------.K----------.-------.F....T..L.....G......I.
atp1b2a .S.TKEED----------RKGS-----SE----------.R----------D-------SF..PRTH.L....AK..GL.LL.
atp1b2b ..--KDGE----------K--------.D----------.K----------E-------.I..PRT.......AS..GL..V.
atp1b3a .--ASTED----------KAAT..ENASS----------.K----------DT-------FY.PRTG.V....AS..AL.LL.
atp1b3b .KEEPEQD----------KKDGK.EETKE----------MK----------ETKESFMDSIY.TRSG......AR..GL..L.
atp1b4 .EPSSTEGGAEETLPKNHPPRPPHKVILKHGQELEEEQEELAEHQPLEQEDLNFER.KRRPLPRRTLHQKIADLKTYL..A.TN..M..S.K..SL.LL.
atp1b1a YLIFYGCLAGIFIGTIQALLLTLSNYKPTYQDRVAPPGLSHTPRSEKS-EIAYTRTEPSTYMPYVESMRKLLEPYEAAVQTDAMKFEDCGGVPKTYTDRG
atp1b1b ..V..............I......W..................-.M.FDPRD.E..L..TKALKNFMSK.DEEG.K.Q.......EH.AE.KN..
atp1b2a .....LF...M.TL.MYM.....DD....W...LTT..MMIR.KGDQ-L..V.SISDKESWDSF.QNLNTF.S..NDTY.VQTN--DN.P-PDQYFIQED
atp1b2b ..V..IF...L.AL.MYVM.Q..DDH...W...LST..MVM..KTDETF..I..VQDTESWDI.TQTLE.F.SS.NES..VQKN--.E.V-PDQYFEQKD
atp1b3a ..V..CF...M.AL.MWVM....DD.V.R.R...PY...VIR.---S.LDMIVNKS..LK.AE..KQLELF.QR.NDTE.-ETN--KE.I-SGNYFLQDN
atp1b3b .....AL...L.LL.MWVM.Q..DENV.R..E...N...VIC.---HAE..SFNHS..AS.TQ.IQQ.NH..QQ.NDS..-AHN--DL.L-.GQF--TEQ
atp1b4 .AAL.LF..AM.G.CMFC.MWSI.P.H..FN...M...MTMA.HLQ-GHD..FNASDRKSWKK.AR..DEY.R..NDGA.ERKNM--R.THAG-YFMQDN
atp1b1a GLDNALGQRMACRFSKSWLGSCSGESDDSFGFREGNPCLIVKLNRIVNFKPRVPTDNGSLPAALQTNQSPNVIPIHCKNKREEDVNKVGPISYFGLGGGF
atp1b1b D.EMDV.V.K....PRTL..P...LE.TE...K..K..V.........F..A.ST.D.I.EEA.PKVQ..L...Y.T......AG.I.E.K.Y.I.E..
atp1b2a SEEVRNNPKRS.Q.NRTI.ED...M..S.Y..NS.Q..ILI....VI.ML.GKDGQSPY---------------VT.GA...DSD-.I..LA..PPN.T.
atp1b2b SG.VKNNPKRS.Q.NRTM..D...LH.RYY.YNL.K..I.I....VIGML.GKDGQAPY---------------.T.GA...DTN-.I.ELE..PPN.T.
atp1b3a AEQM---EKKV...KRDS.SF...L..TN..YS..R..VLL.....IGLM..---G.PY---------------.N.TV.KDSQI-Q---MQ..PSE.LI
atp1b3b NDEP---TKKV.Q.KR.I.QQ...H......AD.K..V...M..VIGL...---G.PY---------------.N.TA..DSPL-H---MQ..PTE.LL
atp1b4 LEES--AE.K..Q.KR....D...LQ.PHY.YSQ.R..VLLRM...LG----------Y..GEGKP------VNVT.GV.KG-PAEAL.EVQF.P-KSI.
atp1b1a PLHYYPYYGKLLHPQYLQPLVAIQF--TNLTLDEEIRIECKVYG-ENIDYS-EKDRYQGRFDVKFTIKS.
atp1b1b ..Q.....L..--...RNM.L......F.-D.....-.........I..QVNGL.
atp1b2a N.M.....KSQVN.T.....VK.L--.AS.NTD.NV...IN-SNTLAVGS.R.KFA..VSF.LR.NDK.
atp1b2b N.M.F....KAQVN.S.....K.L--.V.ANQDVN....IN-AN..PIGS.R.KFA..VSF.LR.N.K.
atp1b3a DKM.F....KA.EN.V.....VKLLLNKEDYNK.LAV..R.E.S-DLRNND.R.KFL..ITFRI.VVE.
atp1b3b DKM.F....KA..E.V.....VKLFL.KEDFNV.QA...R.E.S.DLRNDDSR.KF...VSFRVKVSE.
atp1b4 D.K.....R.GN.SA.V..VR.--ASVQY.SH.QVQ..LN.-KG.INDSPT...L.SVTFSLEV-GA.

Figure 2

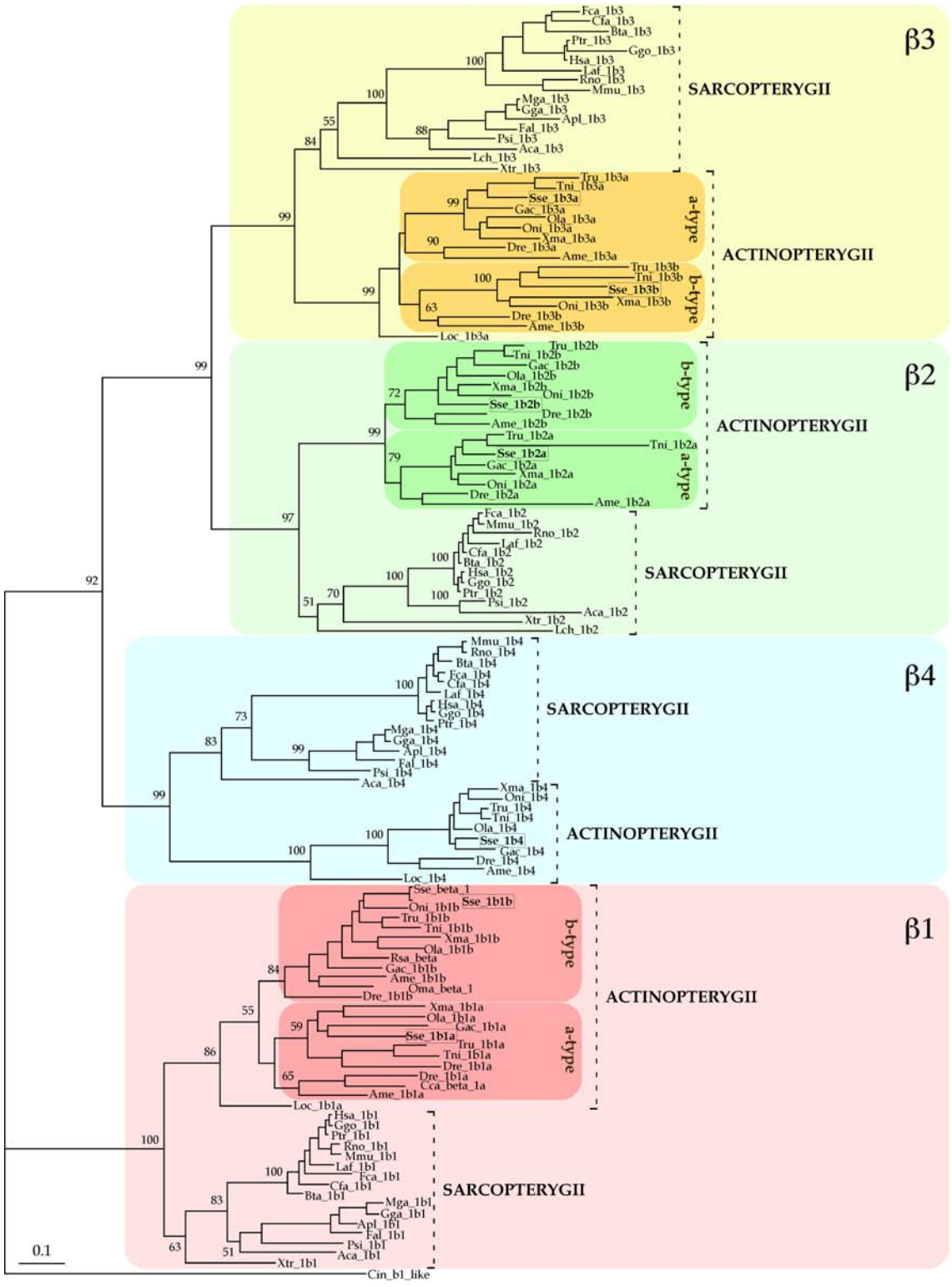
β3
SARCOPTERYGII
ACTINOPTERYGII
a-type
b-type
Fca_1b3
Cfa_1b3
Bta_1b3
Ptr_1b3
Ggo_1b3
Hsa_1b3
Laf_1b3
Rno_1b3
Mmu_1b3
Mga_1b3
Gga_1b3
Apl_1b3
Fal_1b3
Psi_1b3
Aca_1b3
Lch_1b3
Xtr_1b3
Tru_1b3a
Tni_1b3a
Sse_1b3a
Gac_1b3a
Ola_1b3a
Oni_1b3a
Xma_1b3a
Dre_1b3a
Ame_1b3a
Tru_1b3b
Tni_1b3b
Sse_1b3b
Oni_1b3b
Xma_1b3b
Dre_1b3b
Ame_1b3b
Loc_1b3a
β2
SARCOPTERYGII
ACTINOPTERYGII
b-type
a-type
Tru_1b2b
Tni_1b2b
Gac_1b2b
Ola_1b2b
Xma_1b2b
Oni_1b2b
Sse_1b2b
Dre_1b2b
Ame_1b2b
Tru_1b2a
Tni_1b2a
Sse_1b2a
Gac_1b2a
Xma_1b2a
Oni_1b2a
Dre_1b2a
Ame_1b2a
Fca_1b2
Mmu_1b2
Rno_1b2
Laf_1b2
Cfa_1b2
Bta_1b2
Hsa_1b2
Ggo_1b2
Ptr_1b2
Psi_1b2
Aca_1b2
Xtr_1b2
Lch_1b2
β4
SARCOPTERYGII
ACTINOPTERYGII
Mmu_1b4
Rno_1b4
Bta_1b4
Fca_1b4
Cfa_1b4
Laf_1b4
Hsa_1b4
Ggo_1b4
Ptr_1b4
Mga_1b4
Gga_1b4
Apl_1b4
Fal_1b4
Psi_1b4
Aca_1b4
Xma_1b4
Oni_1b4
Tru_1b4
Tni_1b4
Ola_1b4
Sse_1b4
Gac_1b4
Dre_1b4
Ame_1b4
Loc_1b4
β1
SARCOPTERYGII
ACTINOPTERYGII
b-type
a-type
Sse_beta_1
Sse_1b1b
Oni_1b1b
Tru_1b1b
Tni_1b1b
Xma_1b1b
Ola_1b1b
Rsa_beta
Gac_1b1b
Ame_1b1b
Oma_beta_1
Dre_1b1b
Xma_1b1a
Ola_1b1a
Gac_1b1a
Sse_1b1a
Tru_1b1a
Tni_1b1a
Dre_1b1a
Dre_1b1a
Cca_beta_1a
Ame_1b1a
Loc_1b1a
Hsa_1b1
Ggo_1b1
Ptr_1b1
Rno_1b1
Mmu_1b1
Laf_1b1
Fca_1b1
Cfa_1b1
Bta_1b1
Mga_1b1
Gga_1b1
Apl_1b1
Fal_1b1
Psi_1b1
Aca_1b1
Xtr_1b1
Cin_b1_like
0.1

1036 **Figure 3**

1037

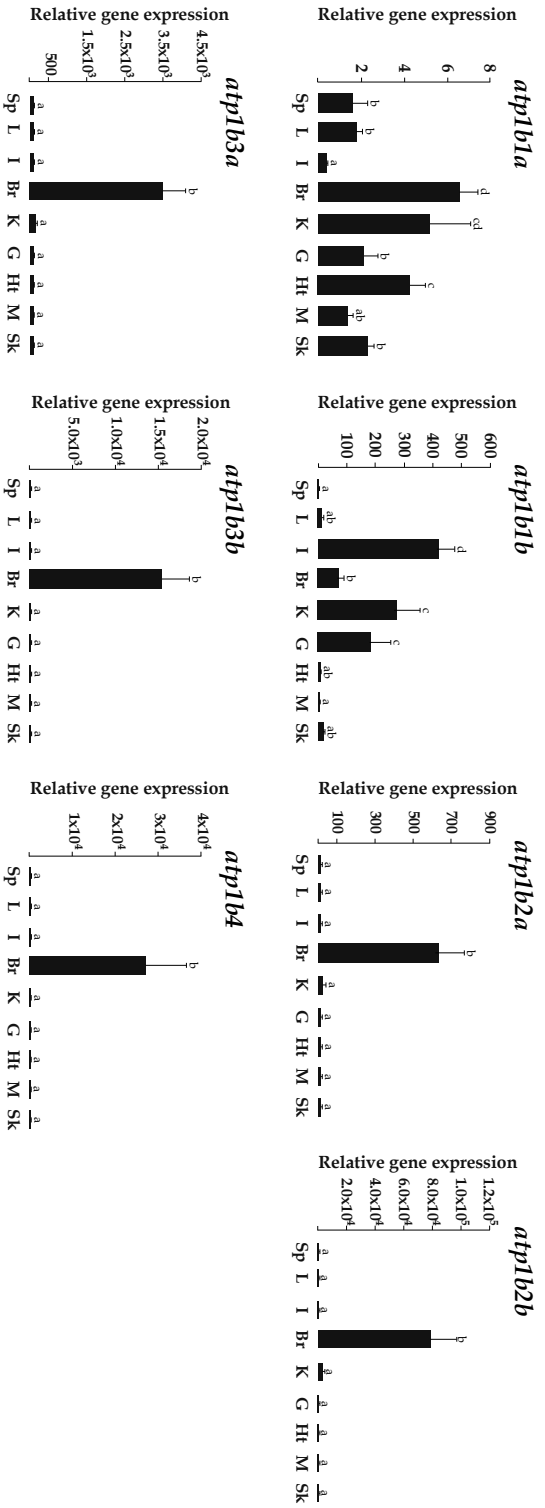

1038

1039

1040

1041 **Figure 4**

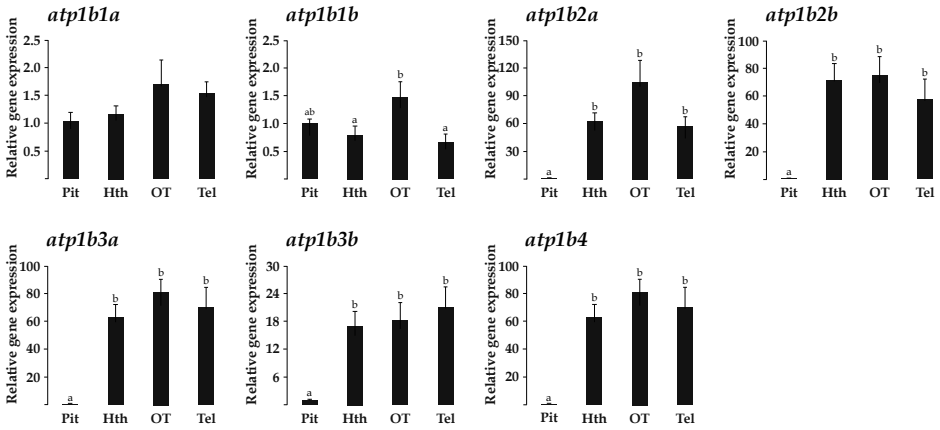

1042

1043

1044 **Figure 5**

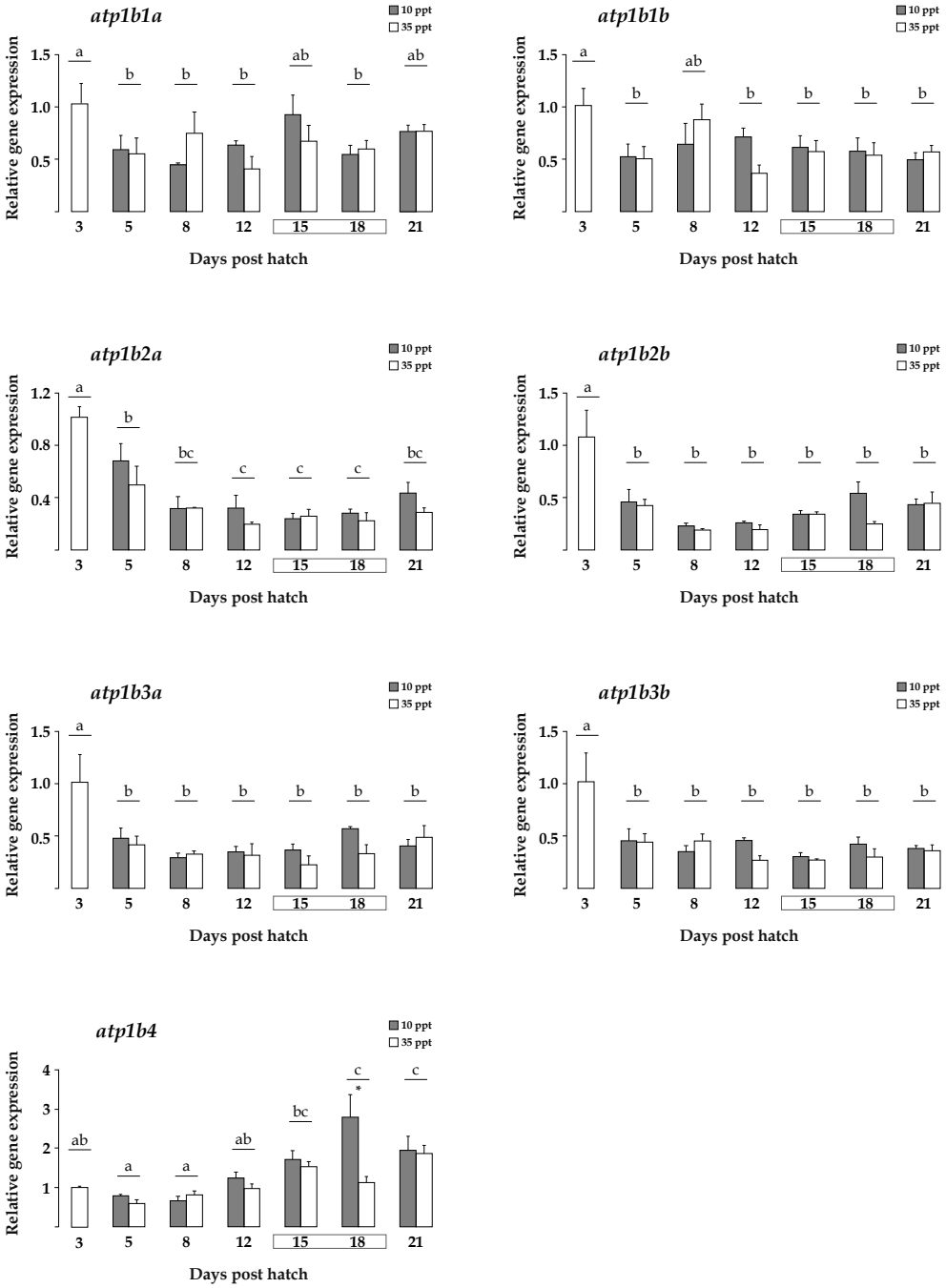

1045

1046

1047 **Figure 6**

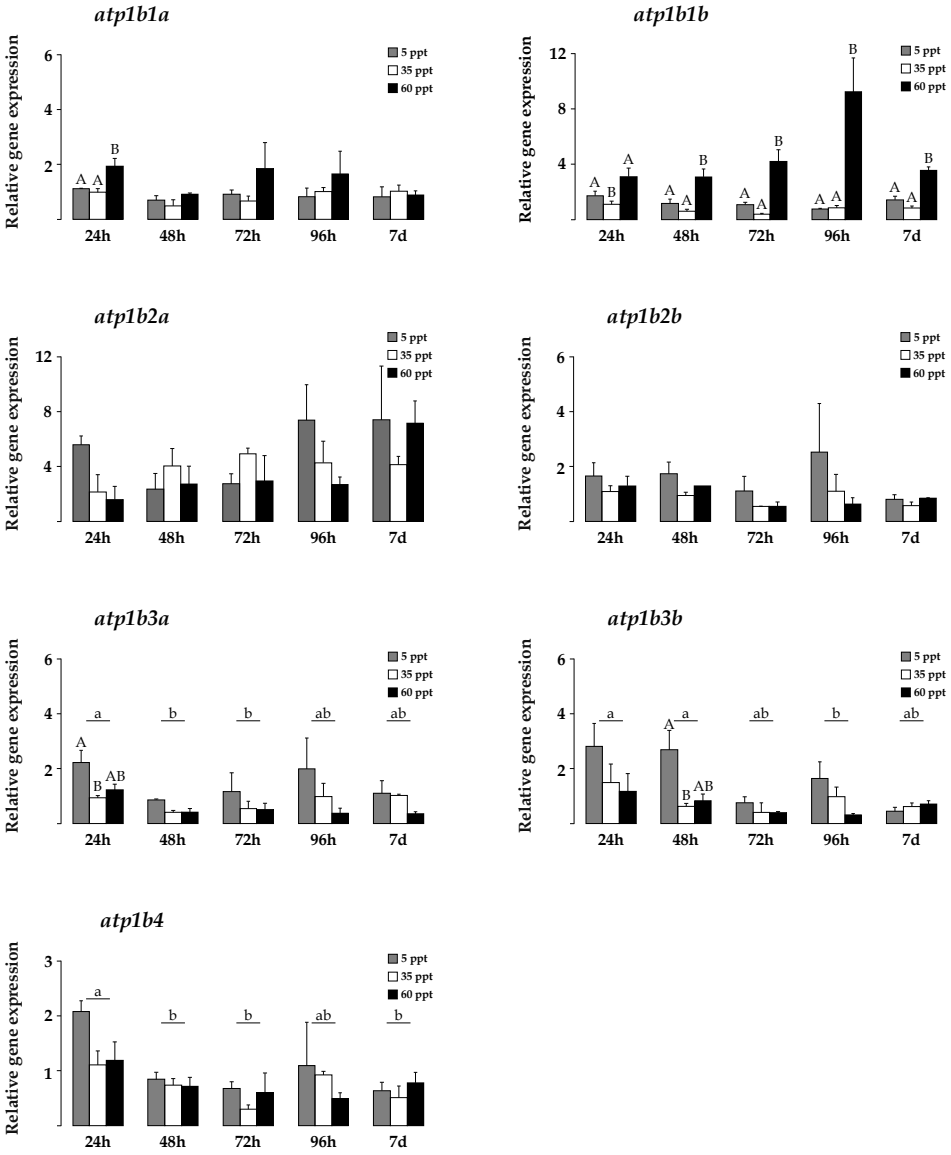

1048

1049

1050 **Figure 7**

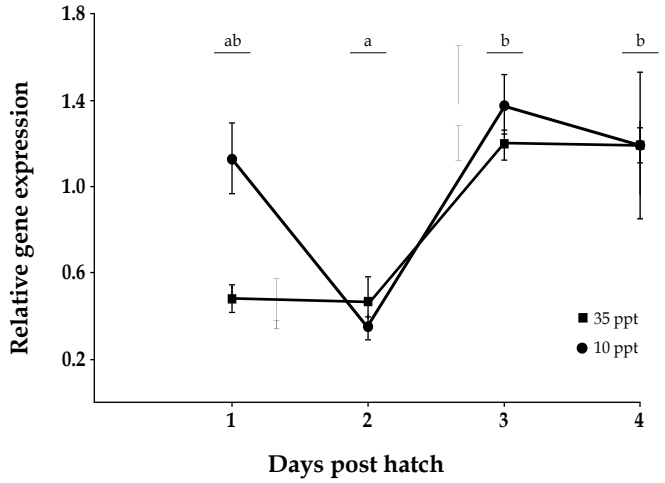

1051

1052

Figure 8

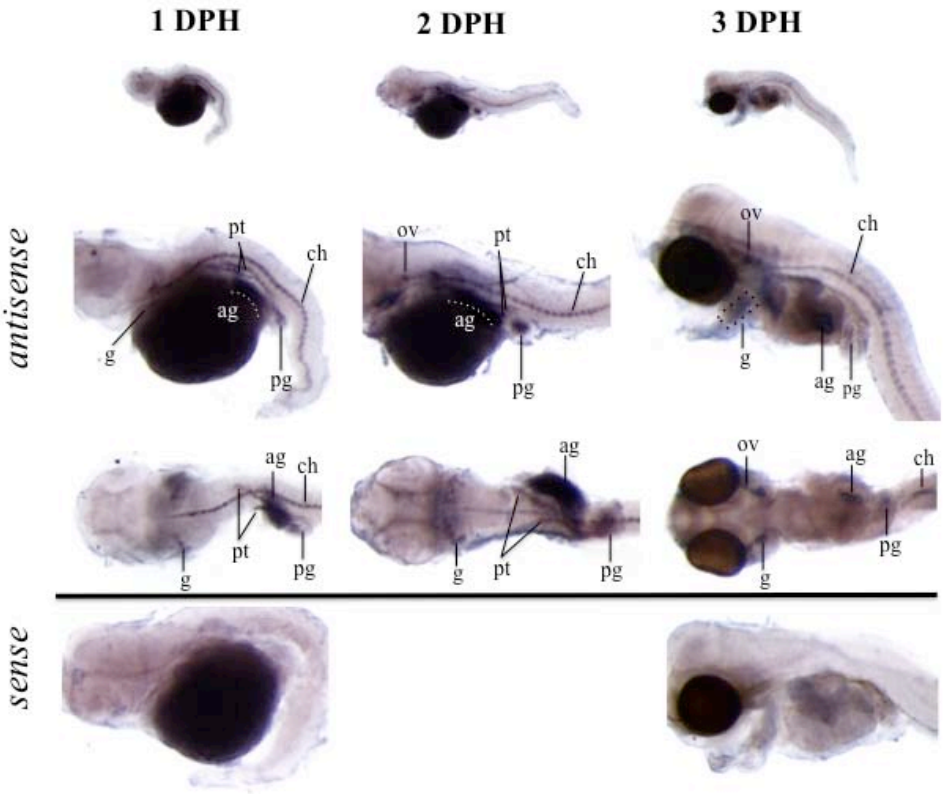

Table 1. List of primers used for qPCR.

Target gene	Sequence	Amplicon size (bp)
atp1b1a	5'-CTTAGGCGGTGGCTTCCCCCTG- 3' (F) 5'- CTTTGCACTCGATGCGGATCTCCTCA-3' (R)	134
atp1b1b	5'- GCAGTTCACCAACCTGACCCGAAAC-3' (F) 5'-ACCTGGAACTTGATGTCAAAGCGTCCC -3' (R)	120
atp1b2a	5'- CTGGCGGGAATGTTCACACTCACC-3' (F) 5'- CGCCCTTTGGACGAATCATCATGC-3' (R)	115
atp1b2b	5'- GTGTGTCCCCGACCAGTACTTTGAGCAG-3' (F) 5'- CAGCATCCCAATCACCCGATTCAGC-3' (F)	184
atp1b3a	5'- TGGCCGTGAAGCTGCTGCTCAA-3' (F) 5'- GGCCGTCTCCTCCTTTACTCCACCAC-3' (R)	160
atp1b3b	5'-TGAACAGAACGATGAGCCCACCAAGAA-3' (F) 5'-CGAGGTTTCAGTCCAATCACCCGATTC-3' (R)	153
atp1b4	5'- CCACCACGTCCGCCTCACAAAGT-3' (F) 5'- GCCTGCGCTTCCATCTCTCAAAGTTCA-3' (R)	127

F and R refer to forward and reverse primers, respectively; bp, base pairs.

Additional file1: List of NKA β subunit sequences used in this study.

The species name, code and accession number are indicated in each case

Species	Code	Accession No.
Anas platyrhynchos	Apl_1b1	ENSAPLG00000016349
	Apl_1b3	ENSAPLG00000006065
	Apl_1b4	ENSAPLG00000009021
Anolis carolinensis	Aca_1b1	ENSACAG00000010651
	Aca_1b2	ENSACAG00000014375
	Aca_1b3	ENSACAG00000005114
	Aca_1b4	ENSACAG00000003749
Astyanax mexicanus	Ame_1b1a	ENSAMXG00000011833
	Ame_1b1b	ENSAMXG00000004723
	Ame_1b2b	ENSAMXG00000006958
	Ame_1b3a	ENSAMXG00000018403
	Ame_1b3b	ENSAMXG00000010219
	Ame_1b4	ENSAMXG00000000205
Bos taurus	Bta_1b1	ENSBTAG00000002688
	Bta_1b2	ENSBTAG00000013680
	Bta_1b3	ENSBTAG00000014140
	Bta_1b4	ENSBTAG00000008920
Canis lupus familiaris	Cfa_1b1	ENSCAFG00000015258
	Cfa_1b2	ENSCAFG00000016703
	Cfa_1b3	ENSCAFG00000007731
	Cfa_1b3	ENSCAFG00000018484
Ciona intestinalis	Cin_b1_like	ENSCING00000007867
Cyprinus carpio	Cca_beta_1a	JX228173
Danio rerio	Dre_1b1a	ENSDARG00000013144
	Dre_1b1b	ENSDARG00000076833
	Dre_1b2a	ENSDARG00000013605
	Dre_1b2b	ENSDARG00000034424
	Dre_1b3a	ENSDARG00000015790
	Dre_1b3b	ENSDARG00000042837
	Dre_1b4	ENSDARG00000053262
Felis catus	Fca_1b1	ENSFCAG00000009332
	Fca_1b2	ENSFCAG00000009622
	Fca_1b3	ENSFCAG00000030431
	Fca_1b4	ENSFCAG00000014941
Ficedula albicollis	Fal_1b1	ENSFALG00000005722
	Fal_1b3	ENSFALG00000006985
	Fal_1b4	ENSFALG00000001546
Gallus gallus	Gga_1b1	ENSGALG00000015233
	Gga_1b3	ENSGALG00000002764
	Gga_1b4	ENSGALG00000008593
Gasterosteus aculeatus	Gac_1b1a	ENSGACG00000013647
	Gac_1b1b	ENSGACG00000015312
	Gac_1b2a	ENSGACG00000001175
	Gac_1b2b	ENSGACG00000020390
	Gac_1b3a	ENSGACG00000015750
	Gac_1b4	ENSGACG00000017418
Gorilla gorilla gorilla	Ggo_1b1	ENSGGOG00000002499
	Ggo_1b2	ENSGGOG00000002715
	Ggo_1b3	ENSGGOG00000027111
	Ggo_1b4	ENSGGOG00000006495
Homo sapiens	Hsa_1b1	ENSG00000143153
	Hsa_1b2	ENSG00000129244

	Hsa_1b3	ENSG00000069849
	Hsa_1b4	ENSG00000101892
Latimeria chalumnae	Lch_1b2	ENSLACG00000011485
	Lch_1b3	ENSLACG00000005279
	Loc_1b1a	ENSLOCG00000008556
Lepisosteus oculatus	Loc_1b3a	ENSLOCG00000008025
	Loc_1b4	ENSLOCG00000015247
	Laf_1b1	ENSLAFG00000013066
Loxodonta africana	Laf_1b2	ENSLAFG00000023256
	Laf_1b3	ENSLAFG00000010553
	Laf_1b4	ENSLAFG00000003704
	Mga_1b1	ENSMGAG00000014349
Meleagris gallopavo	Mga_1b3	ENSMGAG00000006163
	Mga_1b4	ENSMGAG00000007633
	Mmu_1b1	ENSMUSG00000026576
Mus musculus	Mmu_1b2	ENSMUSG00000041329
	Mmu_1b3	ENSMUSG00000032412
	Mmu_1b4	ENSMUSG00000016327
Oncorhynchus masou	Oma_beta_1	AB573641
	Oni_1b1a	ENSONIG00000019331
	Oni_1b1b	ENSONIG00000003739
	Oni_1b2a	ENSONIG00000006654
Oreochromis niloticus	Oni_1b2b	ENSONIG00000004231
	Oni_1b3a	ENSONIG00000010624
	Oni_1b3b	ENSONIG00000014843
	Oni_1b4	ENSONIG00000002552
	Ola_1b1a	ENSORLG00000015696
Oryzias latipes	Ola_1b2b	ENSORLG00000008071
	Ola_1b3a	ENSORLG00000004703
	Ola_1b4	ENSORLG00000001069
	Ptr_1b1	ENSPTRG00000001653
Pan troglodytes	Ptr_1b2	ENSPTRG00000008701
	Ptr_1b3	ENSPTRG00000015476
	Ptr_1b4	ENSPTRG00000022238
	Psi_1b1	ENSPSIG00000002188
Pelodiscus sinensis	Psi_1b2	ENSPSIG00000013357
	Psi_1b3	ENSPSIG00000007680
	Psi_1b4	ENSPSIG00000017687
	Rno_1b1	ENSRNOG00000002934
Rattus norvegicus	Rno_1b2	ENSRNOG00000011227
	Rno_1b3	ENSRNOG00000011501
	Rno_1b4	ENSRNOG00000007059
Rhabdosargus sarba	Rsa_beta	AY553206
Solea senegalensis	Sse_beta_1	JX508625
	Tru_1b1a	ENSTRUG00000004970
	Tru_1b1b	ENSTRUG00000005896
	Tru_1b2a	ENSTRUG00000005213
Takifugu rubripes	Tru_1b2b	ENSTRUG00000016164
	Tru_1b3a	ENSTRUG00000000740
	Tru_1b3b	ENSTRUG00000017963
	Tru_1b4	ENSTRUG00000010323
	Tni_1b1a	ENSTNIG00000013777
	Tni_1b1b	ENSTNIG00000014477
Tetraodon nigroviridis	Tni_1b2b	ENSTNIG00000011776
	Tni_1b3a	ENSTNIG00000007841
	Tni_1b4	ENSTNIG00000015768
	Xtr_1b1	ENSXETG00000002414
Xenopus tropicalis	Xtr_1b2	ENSXETG00000025056

	Xtr_1b3	ENSXETG00000014751
Xiphophorus maculatus	Xma_1b1a	ENSXMAG00000016407
	Xma_1b1b	ENSXMAG00000009766
	Xma_1b2a	ENSXMAG00000011085
	Xma_1b2b	ENSXMAG00000011811
	Xma_1b3a	ENSXMAG00000004371
	Xma_1b3b	ENSXMAG00000013010
	Xma_1b4	ENSXMAG00000013654

Additional file 2: Coding sequence length (nt) of NKA β paralogous genes in *S. senegalensis* (Sse). ORF length for paralogs found in *D. rerio* (Dre), *G. aculeatus* (Gac), *T. rubripes* (Tru) and *O. niloticus* (Oni) are shown. "--" indicates that this paralog was not found. Accession numbers are shown in Additional file 1.

	Sse	*Dre*	*Gac*	*Tru*	*Oni*
atp1b1a	906	921	906	903	885
atp1b1b	906	909	903	906	909
atp1b2a	867	858	861	882	867
atp1b2b	855	879	882	903	858
atp1b3a	843	837	840	840	837
atp1b3b	867	828	--	885	999
atp1b4	1,029	1,044	1,029	1,011	1017

Additional file 3

Percentage of amino acid (above diagonal) and DNA (below diagonal) sequence identity among Senegalese sole (Sse), *Danio rerio* (Dre), and *Oryzias latipes* (Ola) NKA β subunits. The nomenclature 1a, 1b, 2a, 2b, 3a, 3b and 4 refer to the NKA β isoform. Comparisons between *S. senegalensis* isoforms are shaded. Comparisons to *D. rerio* and *O. latipes* NKA β isoforms are separated by a line.

	Sse1a	**Sse1b**	**Sse2a**	**Sse2b**	**Sse3a**	**Sse3b**	**Sse4**	**Dre1a**	**Dre1b**	**Dre2a**	**Dre2b**	**Dre3a**	**Dre3b**	**Dre4**	**Ola1a**	**Ola1b**	**Ola2a**	**Ola3a**	**Ola4**
Sse1a		65.9	33.2	34.7	28.8	31.8	26.8	66.6	64.9	33.2	35.5	29.0	31.2	27.2	67.5	63.4	32.1	28.8	27.5
Sse1b	64.5		33.2	37.9	30.6	28.4	26.8	62.9	70.2	36.4	34.5	25.8	32.2	28.5	66.6	83.5	33.1	27.4	27.5
Sse2a	34.1	38.3		66.7	39.1	35.6	34.6	33.6	35.3	73.4	67.1	39.8	39.5	36.7	35.6	32.3	65.7	39.5	35.6
Sse2b	37.0	42.6	63.4		37.0	37.5	32.3	35.4	37.2	68.1	70.9	38.4	40.9	37.9	36.5	36.0	77.5	39.9	34.0
Sse3a	33.7	34.0	40.0	40.8		56.2	31.3	29.5	28.8	40.9	39.5	63.4	65.9	33.1	29.5	27.4	38.1	74.0	30.6
Sse3b	35.6	31.9	38.9	41.6	55.8		25.6	28.7	30.4	37.4	38.1	60.9	57.2	27.3	29.8	29.3	36.7	54.8	27.0
Sse4	30.1	37.6	39.8	38.9	37.6	31.7		25.7	29.0	34.3	32.8	30.5	32.2	72.2	28.7	25.6	31.9	31.0	90.4
Dre1a	63.2	60.2	34.9	37.1	33.8	31.9	29.5		65.0	35.7	34.5	25.8	30.1	26.4	59.1	62.2	33.2	29.5	25.7
Dre1b	61.3	68.8	39.2	43.4	33.7	33.4	35.8	62.4		35.0	34.1	28.7	32.2	30.0	63.0	69.5	36.0	30.6	30.4
Dre2a	40.1	41.5	69.5	64.6	41.8	40.2	39.9	35.8	37.3		71.0	39.8	40.6	36.0	35.3	33.5	67.5	41.3	36.7
Dre2b	37.5	41.4	64.7	68.5	38.2	37.1	35.7	37.2	36.3	68.6		40.1	42.8	36.2	34.1	33.5	72.0	41.6	34.8
Dre3a	29.9	34.1	37.2	39.1	61.4	57.2	36.0	29.5	29.6	39.1	38.0		66.7	32.3	28.3	29.3	39.8	64.9	31.5
Dre3b	33.3	33.9	41.4	42.9	61.5	57.0	35.9	31.5	33.2	42.9	43.2	62.0		34.1	31.2	27.4	40.2	63.4	33.7
Dre4	35.1	34.1	40.1	42.6	35.7	33.2	66.8	28.7	33.2	38.6	39.2	36.1	34.9		28.4	29.9	36.8	32.7	73.5
Ola1a	69.2	61.6	39.6	41.1	36.5	33.3	34.7	58.4	61.1	37.3	37.5	32.3	36.1	33.0		67.1	31.4	30.2	30.0
Ola1b	62.8	78.9	39.0	35.2	35.0	33.1	32.7	60.0	67.7	34.3	34.8	31.9	27.6	35.0	62.6		34.8	28.7	25.0
Ola2a	34.4	38.1	63.2	77.4	41.4	36.6	37.3	37.8	36.4	64.8	67.0	40.3	43.8	40.6	34.5	38.4		40.9	33.9
Ola3a	34.0	37.0	41.6	43.5	74.7	55.8	37.0	32.9	36.3	41.9	42.5	61.5	58.7	38.1	36.1	33.5	39.9		30.6
Ola4	30.2	34.8	39.9	38.8	36.4	29.4	85.8	29.6	34.8	41.0	39.1	34.9	36.7	65.2	35.3	33.1	36.7	36.5	

1110